Transportation Research Part C 137 (2022) 103563

Contents lists available at ScienceDirect

Transportation Research Part C

journal homepage: www.elsevier.com/locate/trc

Two-stage robust facility location problem with drones

Tengkuo Zhu [a,*], Stephen D. Boyles [a], Avinash Unnikrishnan [b]

[a] University of Texas at Austin, TX, United States of America
[b] Portland State University, Portland, OR, United States of America

ARTICLE INFO

Keywords:
Robust optimization
Facility location problem
Drone delivery

ABSTRACT

The past few years have witnessed the increasing adoption of drones in various industries such as logistics, agriculture, military, and telecommunications. This paper considers a short-term post-disaster unmanned aerial vehicle (UAV) humanitarian relief application where first-aid products need to be delivered to the customer demand points. The presented problem, two-stage robust facility location problem with drones (two-stage RFLPD), incorporates the demand uncertainty using demand scenarios. This problem aims to find a location–allocation-assignment plan that has minimal two-stage total cost in the worst-case scenario of all the possible demand outcomes. Three different models of the problem are proposed, two of which incorporate a realistic UAV electricity consumption model while the last one has greater operational flexibility. The column-and-constraint generation method and Benders decomposition are used to solve the two models, and a thorough comparison among the deterministic facility location problem with drones (FLPD) models and three proposed models are also presented. Numerical analysis results show that the proposed model has significantly less average cost in the simulation runs compared to the deterministic FLPD.

1. Introduction

The past few years have witnessed the increasing adoption of drones in various industries such as logistics, agriculture, military, and telecommunications. According to Bloomberg (Bloomberg, 2019), the market value of drone package delivery is estimated to reach US $27.4 billion by 2030. There are several reasons why drone delivery is becoming popular in the logistics industry. First, the rapid deployment ability of drones indicates that the delivery tasks could be performed without a costly truck operator. Second, drones are unaffected by congestion in-ground traffic; this is especially important for time-sensitive deliveries, as in medical logistics. Third, drone delivery produces fewer carbon dioxide emissions than delivery with conventional internal combustion engines and petroleum-fuel powered vehicles (Goodchild and Toy, 2018). As a result, major companies such as Amazon, Google, and DHL have announced initiatives to deliver parcels with drones. Moreover, the ongoing COVID-19 pandemic has also fueled the rise of the no-contact drone-based delivery method as an alternative to traditional methods (Walmart, 2020).

Drone delivery projects are quickly expanding around the globe. According to UnmannedAirspace (2020), more than 27 countries have established, are testing, or are planning to test this new delivery method. Specifically, the recent successful UAV application in humanitarian aid tasks, that is, delivering medical supplies to remote or hard-to-access areas, has caught attention in industry and academia. In May 2016, Zipline, a US robotics and drone company, started the world's first commercial drone delivery service in Rwanda to deliver blood and blood products. During the operation, local health workers can request a blood drop via text message, and the UAV can fulfill this request in 30 min by dropping blood parcels on parachutes outside remote health centers (Dronezone, 2020).

* Corresponding author.
E-mail addresses: zhutengkuo@utexas.edu (T. Zhu), sboyles@mail.utexas.edu (S.D. Boyles), uavinash@pdx.edu (A. Unnikrishnan).

https://doi.org/10.1016/j.trc.2022.103563
Received 17 May 2021; Received in revised form 7 October 2021; Accepted 12 January 2022
Available online 24 February 2022
0968-090X/Published by Elsevier Ltd.

A challenge associated with drone delivery is that payloads are restricted in weight and volume. Based on UnmannedCargo (2016), the average payload capacity of currently-available commercial drones is approximately 4.8 lbs (2.2 kg). According to Wing and Zipline, two leading companies in the UAV delivery industry, their service payload capacity is around 3.85 lbs (1.75 kg). Although recent progress in UAVs' propulsion system makes it possible for some high payload drones to carry packages up to 17 lbs (AirborneDrones, 2020), in the foreseeable future, it is still likely that commercial UAV can only be able to serve one customer before being reloaded at a depot. One way to address this issue is to build drone hub facilities or depots (which we term *warehouses*) that are close to the customers. The drone departs from the warehouse and travels to customer locations in the delivery process. The parcel is then dropped off near the customer's front door, and the drone returns to the warehouse, without human intervention (Chowdhury et al., 2017; Chauhan et al., 2019).

This paper considers a short-term post-disaster humanitarian relief application where first-aid products (such as blood products or medicines) must be delivered to customer demand points (e.g., health centers). Multiple warehouses, which serve as both distribution centers and drone launch/retrieve hubs, need to be built before the delivery operation is adopted. As a result, the problem is divided into two stages, the *strategic* planning stage and the *operational* stage. In the strategic planning stage, the planner must decide the location of the warehouses and the allocation of the drones to the opened facilities. Meanwhile, we further assume that the exact demand value at each health center is unknown when the warehouses are built. Instead, the planner is given a set of estimated nominal demand values of each health center. In the operational stage, the realized demand values at the health centers are revealed, and the planner must assign customers to warehouses, and UAVs to customers, to satisfy this demand. The UAVs' flight range, battery, and payload capacity must be considered. We model demand stochasticity by scenarios, each of which represents one possible outcome. This paper uses a cardinality constraint set to restrict the number of sites where disruption occurs. The objective is to find a location–allocation-assignment plan with a minimal two-stage total cost in the worst-case scenario of all the possible demand outcomes. This problem is named the two-stage robust facility location problem with drones (two-stage RFLPD).

We propose three different two-stage RFLPD models which adopt different drone electricity consumption functions under various delivery assumptions. The first two models incorporate realistic UAV electricity consumption functions but prohibit split delivery in the operational process. The last model uses a slightly simplified UAV electricity consumption function but has more operational flexibility. The column-and-constraint generation (C&CG) method and Benders decomposition are used to solve the models. The numerical analysis section presents a thorough comparison among all three proposed models and two additional deterministic FLPD models.

The remainder of this paper is structured as follows. Section 2 discusses previous work that addresses the facility location problem under uncertainty and drone routing in logistics. Section 3 describes the problem in full detail and proposes three models with various assumptions. Section 4 introduces different solution methods used to solve these RFLPD models. Section 5 compares these models extensively and reports the experimental results based on randomly generated instances. Finally, Section 6 presents conclusions and future work.

2. Literature review

As RFLPD involves both FLP and drone operation, this section consists of two parts. The first part presents related FLP papers that involve multiple-period planning or consider parameter uncertainties, while the second part reviews papers that involve drone operation, especially in logistics.

2.1. FLP models

As the central problem of location science, the facility location problem has become an active research area that is highly interconnected with multiple disciplines and has various applications in many fields. The origin of this problem dates to the 17th century as a geometric problem of finding a point minimizing the sum of its distances to three fixed points. The extension of this problem to the multi-facility case in the 1960s marked a new era. Significant progress has been made in the past 60 years. Nowadays, this problem has been applied to many areas with great success, such as logistics (Shavarani, 2019; Lu and Bostel, 2007; Daskin et al., 2005), telecommunications (Fischetti et al., 2004; Kim and O'Kelly, 2009; An et al., 2017), routing (Balakrishnan et al., 1987; Cappanera et al., 2003) and transportation (Ouyang et al., 2015; Hajibabai et al., 2014). Different FLP models exist in various fields, the most important ones being set-covering, $p-$median, $p-$center, and fixed charge facility location models. As in many other problems, these models can also be divided into two categories based on whether uncertainties are considered: deterministic FLP and FLP with uncertainties. A variety of researchers have studied the deterministic facility location problem. For a full review, we refer the reader to the surveys by Owen and Daskin (1998) and Melo et al. (2009).

Many FLP models incorporate uncertainties, as facility location generally involves strategic decisions over a longer period, and there may be changes in demands, cost, capacity, or other parameters during the facilities' operating lifetime. Some examples of the review papers of FLP problems under uncertainty include Louveaux (1993), Snyder (2006), Melo et al. (2009), and Correia and Saldanha-da Gama (2019). As described in Shen et al. (2011), in general, the uncertainties can be classified into three categories: provider-side uncertainty, receiver-side uncertainty, and in-between uncertainty. Provider-side uncertainty refers to the uncertainty in facility capacity, facility reliability, and facility availability. Receiver-side uncertainty corresponds to the uncertainty of the customer side, for example, customer presence, demand, and location. In-between uncertainty indicates the uncertainty of the service delivery process. Accounting for these uncertainties in the decision-making process can produce more reliable solutions. When dealing with these uncertainties, different types of models are available. Choosing the most appropriate model typically

requires the agency to consider several factors, such as the representation of the uncertainties, the attitude towards the future risks, and identifying the *ex-ante* and *ex-post* decisions.

A variety of recent works consider provider-side uncertainties in the context of FLP. Drezner (1987) is one of the early works that address facility failures in the p-median and p-center problems. It introduces an "unreliable" p-median problem, where each facility has a given probability of "failure", and (p, q)-center problem, where p facilities are to be located and at most q of them may become inactive. Daskin et al. (2005) proposed the concept of "reliable" p-median FLP and fixed charge FLP that minimizes the sum of the operating cost and the expected failure cost while assuming each facility has the same probability of failing. A similar assumption is also used in Xie et al. (2016), where a location-routing problem is solved. Cui et al. (2010) extends the concept of "reliable" fixed charge FLP by assuming each facility has site-dependent failure distribution and proposes a mixed integer programming formulation and a continuum approximation model. This failure distribution assumption is further relaxed later in Li and Ouyang (2010), in which spatial correlation among facility disruptions is considered in the uncapacitated fixed charge location problem. This work then adopts a continuum approximation model to minimize the sum of construction cost and transportation cost. Xie et al. (2019) presents a reliable FLP model under correlated facility disruption where facility disruption is represented by constructed supporting stations. Shen et al. (2011) solve a scenario-based uncapacitated reliable facility location problem where each scenario is associated with a known probability. Then the problem is formulated as two-stage stochastic programming that minimizes the total cost across two stages.

Many other works account for the receiver-side uncertainties and in-between uncertainties. Mišković et al. (2017) considers a multi-source variant of two-stage capacitated facility location problem, where transportation costs for plant–depot pair and depot–customer pair may increase. Box uncertainties represent the uncertainties in the transportation cost, and a robust optimization MILP model is proposed in the paper. Zetina et al. (2017) presents robust uncapacitated hub location problems in which the customers' demand, transportation cost, or both could be uncertain. Mixed-integer programming formulations are proposed for each case, and a branch-and-cut algorithm is used to solve them. Zeng and Zhao (2013) solved the two-stage robust location-transportation problem. The facilities' location and capacity are determined in the first stage, and the second stage decides the allocation of customers to the facilities. An et al. (2014) addressed the p-median facility location problem to build a reliable network under disruptive scenarios. In a disruptive scenario, the authors assume that a customer's demand might change from its nominal demand value, and a cardinality constrained uncertainty set is used to restrict the total change. The location and initial allocation plan are determined in the first stage, and the allocation plan might change after the actual demand is revealed. The C&CG algorithm is used to solve this problem. Similar to the problem proposed in this paper, Ardestani-Jaafari and Delage (2018) presents a multi-period FLP where the location and capacity of each facility must be determined before exact demand is known. A budget uncertainty set is used to describe demand uncertainty, and a robust optimization approach is adopted. Several approximation models are proposed to estimate the problem solution, and a row generation algorithm is used to solve problem instances of realistic size.

2.2. Drone-related routing problems

Otto et al. (2018) provides a detailed review of models for optimizing drone delivery operations and the various applications. A particular focus of research is the newly emerged truck-drone tandem delivery method, in which a truck serves as the drone hub for reloading the drone and refreshing its battery, while both vehicles perform delivery tasks (Murray and Chu, 2015; Ponza, 2016; Wang et al., 2017; Poikonen et al., 2017; Daknama and Kraus, 2017; Carlsson and Song, 2017; Agatz et al., 2018; Yurek and Ozmutlu, 2018; Ha et al., 2018; Sacramento et al., 2019). Methodologically, these papers involve solving the traveling salesman or vehicle routing problem using trucks or trucks and drones. *In this paper, we focus on drone deliveries only and do not consider truck routing*. Dorling et al. (2017) and Choi and Schonfeld (2017) model multiple deliveries by drones from single depot. *This paper considers the location of multiple drone-launching sites or depots as decision variables. We also allow drones to make multiple depot-to-customer trips if the battery charge is sufficient.*

Similar to this paper, several past researchers, for example, Chowdhury et al. (2017), Golabi et al. (2017), Pulver and Wei (2018), Macias et al. (2020), Ilkhanizadeh et al. (2020), study drone delivery based FLPs. Chowdhury et al. (2017) proposes a location model of determining the location of distribution centers and the supply inventories at these centers in a humanitarian relief scenario under stochastic demand and drone flying range constraints. A continuous approximation (CA) model is presented to solve this model. Golabi et al. (2017) presents a post-disaster FLP problem where the location of distribution centers needs to be decided. In this problem, some network edges might collapse and thus lose their accessibility, and the goal is to minimize the total transportation cost. Pulver and Wei (2018) study a max-coverage model where drones are used to transport medical supplies. Macias et al. (2020) also considers a post-disaster application where both the trajectory of drones and the location of charging stations need to be decided. Ilkhanizadeh et al. (2020) presents an FLP in tourism where drones are used to provide online virtual tours.

Our approach differs from these in several aspects with the papers mentioned above. In Chowdhury et al. (2017), both trucks and drones are used to make deliveries, whereas, in our model, only drones are used. Pulver and Wei (2018) do not consider capacity constraints at facilities. Both Pulver and Wei (2018) and Ilkhanizadeh et al. (2020) do not model the increase in energy consumption with the payload. We model both these aspects. Moreover, Chowdhury et al. (2017) assume one trip per drone, whereas, in our model, drones can make multiple drone deliveries until the battery is depleted. Macias et al. (2020) study a two-stage model for locating uncapacitated hubs and optimizing drone trajectories for relief supply applications. Golabi et al. (2017) study the integration of drones into optimizing relief supply post-disaster from mobile and immobile facilities. Drones are used to satisfy the demand of people living alongside collapsed roadway segments. In this research, we consider the allocation of drones to facilities, which is not considered in the works mentioned above. This research is different from the model proposed by Chauhan et al. (2019, 2020)

in multiple aspects. Both Chauhan et al. (2019) and Chauhan et al. (2020) focus on maximizing coverage, whereas our objective is to minimize cost. Chauhan et al. (2019) do not consider the impacts of uncertainty. Chauhan et al. (2020) considers battery consumption and capacity uncertainty using a robust optimization approach. Our paper focuses on demand uncertainty. Chauhan et al. (2019, 2020) use a three-stage heuristic, whereas we have developed Benders decomposition and C&CG algorithms to solve our model.

Other studies have modeled the impact of uncertainty in drone delivery problems. Kim et al. (2018) model the effect of air temperature on uncertainty in maximum flight duration using robust optimization. However, Kim et al. (2018) do not consider the impact of payload on energy consumption, drone allocation to facilities, and assume facilities to be incapacitated. Kim et al. (2019) model the effect of battery uncertainty using a chance constraint based on exponential distribution. Shavarani et al. (2018) model demand uncertainty using a Poisson distribution. However, in the formulation, the mean demand parameter is used. Shavarani et al. (2019) use a fuzzy variable approach to study the impact of uncertainty in demands, facility opening and drone procurement costs, and drone distance capacity. A genetic algorithm is used to solve the models presented in Shavarani et al. (2018, 2019).

Our paper differs from past research in that we incorporate drone deliveries and allocation into FLP and use an empirically derived electricity consumption function. In the previous works in FLP, the uncertainty of customers' demand only affects the location of the facilities and the allocation of customers to facilities. However, in this work, this randomness also affects drones' operation via electricity consumption and the assignment of customers to drones. Thus, in this model, demand randomness affects the whole location–allocation-assignment process. While several researchers have modeled uncertainty in drone operations, to our knowledge, our approach is the first to adopt a two-stage robust optimization approach on drone-related facility location problems.

3. Problem description and mathematical formulation

In the two-stage RFLPD, we consider a humanitarian relief scenario where an agency wants to deliver first-aid items (such as medicine or blood) to several demand points (also called customers) using the warehouse-drone delivery system after the disaster outbreak. In this delivery system, the warehouses serve both as distribution centers where production can be dispatched and drone hubs for launching/retrieving/refilling a limited number of drones. This problem consists of a strategic planning stage and an operational stage. In the first strategic planning stage, the agency needs to locate warehouses and allocate available drones to the opened warehouses before the exact customers' demands are known. The location and allocation decisions are made with only nominal demand value information, but this should account for the future uncertainties. In the second operational stage, the agency needs to assign the drones to serve the customers, whose actual demands would be revealed by then. Some of the additional assumptions are:

(1) The maximum number of opened facilities is given as a fixed parameter.
(2) We assume the warehouses' capacity is a fixed parameter as they are built after the disaster outbreak
(3) In the operational stage, the drone launches from the warehouse j while carrying a parcel, travels to the customer i assigned to it, delivers the parcel, and returns to the warehouse j before it is refilled and relaunched. This full process of service is called a *drone trip*. Each drone trip involves service to only a single customer.
(4) The drone has a limited load capacity for the parcels it carries.
(5) Each drone is equipped with a fully-charged battery which **cannot** be recharged. It can operate as long as its battery is not fully depleted.
(6) The service radius of drones is assumed to be large enough to cover every customer in the targeted area, which indicates that any available drone can serve any customers in the problem, given that the drone's load capacity and battery capacity constraints are satisfied.

The objective of RFLPD is to obtain a feasible location–allocation-assignment plan such that the total cost is minimized in the worst-case scenario. The total cost includes the fixed cost of opening facilities (first-stage cost), transportation cost of serving customers (second-stage cost), and the penalty cost if a customer's demand cannot be fully satisfied (second-stage cost).

Let I be the set of all the customer nodes, J the set of potential facility locations, and K the set of all the available drones. Denote the nominal demand and actual demand of customer $i \in I$ as w_i and $\tilde{w}_i$, respectively. In RFLPD, we assume that only the nominal demand value is available to the planner in the first stage. The actual demand is only revealed at the beginning of the operational stage after the location–allocation plan has been made. This assumption reflects that the specific disruptions caused by a disaster are not known in advance, even if a "typical" or expected scenario is envisioned. This uncertainty demand assumption is common in many related robust FLP investigations (Cheng et al., 2021; Ardestani-Jaafari and Delage, 2018; Atamtürk and Zhang, 2007). In general, the delay of demand information and uncertainty of the severity of different regions leads to the randomness of the modeling process of RFLPD.

In this research, the customer's actual demand $\tilde{w}_i$ is represented as $\tilde{w}_i = (1 + \theta_i s_i)w_i$. In the above expression, $s_i \in S$ is the disruption indicator variable for site i and $\theta \in [-1, +\infty)$ is a new parameter introduced to capture and characterize these "disrupted" scenarios. Similar to An et al. (2014), s_i is described in a budget set S, which is defined by:

$$S = \{s_i \in [0,1] : \sum_{i \in I} s_i \leq \Gamma\}$$

where Γ is a pre-defined parameter called disruption budget. This parameter represents the maximum number of disruptions that can happen simultaneously in the worst-case scenario. When $s_i = 0$ the actual demand $\tilde{w}_i$ remains at its nominal value in disruption

scenarios. On the other hand, when $s_i = 1$ the actual demand $\tilde{w}_i = (1 + \theta_i)w_i$. Thus, by setting parameter θ_i to a negative value the actual demand will shrink in a disruption scenario and setting θ_i to a positive value indicates the case when the actual demand increase in a disruption scenario. Besides, let c_{ij} represent the unit demand cost of serving i by the facility located in j. There is a fixed cost f_j associated with opening a facility at j.

For the decision variables, let the binary variables y_j indicate whether a facility is opened at j. The binary variables z_{jk} indicate whether drone k is assigned to a facility located at j. Both y_j and z_{jk} are first-stage decision variables. The second-stage decision variables x_{ijk} represent the assignment of drones to customers, where i is the customer index, k the drone index, and j the facility index where the drone is based.

In this paper, we consider a robust two-stage decision-making process. Unlike the traditional one-stage robust optimization, where all the decision variables must be decided before realizing the uncertain data, in this paper, the two-stage decision-making modeling enables some decision variables to be decided after the realization of the uncertain data. The two-stage setting thus can create a more reliable network than the deterministic one-stage robust optimization approach. In our approach, in the first stage, the values of all y_j and z_{jk} must be decided. After the uncertain data are realized, the second-stage decision variables' values x_{ijk} will then be decided.

The full set of notations used in the paper is as below:

Sets

I	:	Set of all customers
J	:	Set of all potential facility locations
K	:	Set of all available drones

Parameters:

Γ	:	Maximum number of disruptions that can happen simultaneously
B	:	Battery capacity of drone
f_j	:	Fixed cost of opening a facility at location $j \in J$
d_{ij}	:	Distance between node $i \in I$ and node $j \in J$
c_{ij}	:	Unit demand cost of serving customer i with facility located at j
r_i	:	Unit demand penalty cost associated with customer i
θ_i	:	Demand change parameter associated with customer i
p	:	Maximum number of opened facilities
U_j	:	Capacity of the facility located at j
C_k	:	load capacity of drone $k \in K$
w_i	:	Nominal demand at customer $i \in I$
$\tilde{w}_i$	:	Actual demand at customer $i \in I$

Decision variables:

$y_j \in \{0,1\}$	:	First-stage decision variable, equals to one if the facility is located at $j \in J$ and 0, otherwise
$z_{jk} \in \{0,1\}$	:	First-stage decision variable, equals to one if the kth drone is assigned to facility $j \in J$ and 0, otherwise
x_{ijk}	:	Second-stage decision variable, which indicates the proportion of the satisfied demand of customer i with drone k located at facility j. We consider cases both where demand cannot be split (binary x_{ijk}) among UAVs, and when it can (continuous x_{ijk}).
s_i	:	Second-stage decision variable, which indicates the worst-case scenario whose cost we aim to minimize.

The basic RFLPD formulation is as below.

RFLPD:

$$\min_{y,z,x,s} \sum_j f_j y_j + \max_s \min_{x \in S(y,z)} \sum_i \sum_j \sum_k c_{ij} \tilde{w}_i x_{ijk} + \sum_i r_i \tilde{w}_i (1 - \sum_j \sum_k x_{ijk}) \tag{1}$$

s.t.

$$\sum_j y_j \le p \tag{2}$$

$$z_{jk} \le y_j \qquad \forall j \in J, k \in K \tag{3}$$

$$\sum_j z_{jk} \le 1 \qquad \forall k \in K \tag{4}$$

$$z_{jk}, y_j \in \{0,1\} \qquad \forall j \in J, k \in K \tag{5}$$

Here $x \in S(y,z)$ is defined by a set of constraints:

$$x_{ijk} \le y_j \qquad \forall i \in I, j \in J, k \in K \tag{6}$$

$$\sum_j \sum_k x_{ijk} \le 1 \qquad \forall i \in I \tag{7}$$

$$\sum_i b_{ij}(\tilde{w}_i x_{ijk}) \le B z_{jk} \qquad \forall j \in J, k \in K \tag{8}$$

$$\sum_i \sum_k (1+\theta_i s_i) w_i x_{ijk} \le U_j y_j \qquad \forall j \in J \tag{9}$$

$$\tilde{w}_i x_{ijk} \le C_k \qquad \forall i \in I, j \in J, k \in K \tag{10}$$

$$0 \le x_{ijk} \le 1 \text{ or } x_{ijk} \in \{0,1\} \qquad \forall i \in I, j \in J, k \in K \tag{11}$$

The objective (1) of RFLPD is to minimize the total fixed facility cost and the worst-case operational cost, which includes the transportation cost of serving customers and the penalty cost if a customer's demand is not satisfied or partially satisfied. In the first stage, constraints (2) indicate that the number of total opened facilities should not exceed the pre-set limit of p. Constraints (3) enforce that a drone can be assigned to a facility j only if the facility located at j is opened. Constraints (4) require that any specific drone can only be assigned to at most one facility. Constraints (5) are decision variable domain constraints.

In the second stage, constraints (6) indicate that serving a customer i with a drone k located at facility j is applicable only when the facility located at j is opened. Constraints (7) ensure that any customer cannot be served more than its demand. Constraints (8) indicate that for any drone k located at facility j, its total consumed electricity should not exceed its capacity. Note that $b_{ij}(\chi)$ represents the electricity consumed when delivering a package of weight χ between node $i \in I$ and $j \in J$; see the discussion below on how this energy cost is calculated. Constraints (9) require that the total weight of packages at facility j should not exceed the facility's capacity. Constraints (11) are decision variable domain constraints.

From a modeling standpoint, we study two main types of RFLPD: either with binary decision variables (representing cases where delivery cannot be split, and a single drone must either serve a customer's demand in full or not at all) or with continuous decision variables (allowing split and partial service). Furthermore, as described below, there are several choices for modeling the amount of electricity consumed when serving a customer. In all, we define six models in the remainder of this section, representing different combinations of these choices. Three of them are intended for practical use, and three others are proposed as benchmarks useful for comparison but either impractical to solve or unrealistic for application.

As detailed in the following subsections, RFLPD-BL and RFLPD-BN are binary models where the electricity consumption functions are respectively based on linear and non-linear models proposed in past literature; both include a fixed energy consumption for making a trip, plus a weight-dependent component.

For continuous models, this fixed term poses difficulties since the electricity consumption has a discontinuity at zero (no service at all means no consumption, but even minimal partial service should include the entire fixed amount). We call such a model the "ideal" model: we know no efficient way to solve it, but it is the most realistic way to model split delivery. We, therefore, propose a continuous model RFLPD-C, using a simplified energy consumption model that only includes a weight-dependent term (no fixed cost) but with a different coefficient that is estimated in a way that tends to be conservative. We can then *evaluate* these solutions using the "ideal" model to calculate how much electricity would be used in the RFLPD-C solutions and verify that the parameter estimation is conservative.

Directly comparing the binary models and RFLPD-C is difficult since there are two significant differences (binary vs. continuous variables and an original vs. simplified electricity consumption function). To disentangle these effects, we propose two additional models that only change one factor: RFLPD-BS is a binary model that uses the simplified consumption function for RFLPD-C, and RFLPD-CL is continuous uses the same consumption function as RFLPD-BL. Both of these models have severe shortcomings, and we do not recommend their use in practical settings: RFLPD-BS uses a simplified consumption model without fixed costs, even though as a binary model, this simplification is unneeded; and RFLPD-CL treats the fixed cost as if it were weight-dependent, underestimating actual battery use. Nevertheless, including results with these latter two models helps demonstrate the impact of each change independently.

The reader may also find it instructive to refer to Table 2 when reading this section and the next.

3.1. Drone's electricity consumption model

Suppose that drone $k \in K$ launches from facility $j \in J$, delivers parcels of weight w_i to demand point $i \in I$ with a cruising speed v^c and then returns to facility j (with the same cruising speed). To estimate the drone's electricity consumption along this trip, its whole flight profile is divided into six phases:

- Take off phase at facility j, whose required time is denoted as τ_j^t
- Cruise phase from facility j to customer i, whose required time is denoted as τ_{ji}^c
- Landing phase at customer i, whose required time is denoted as τ_i^l
- Take off phase at customer i, whose required time is denoted as τ_i^t
- Cruise phase from customer i to facility j, whose required time is denoted as τ_{ij}^c
- Landing phase at facility j, whose required time is denoted as τ_j^l

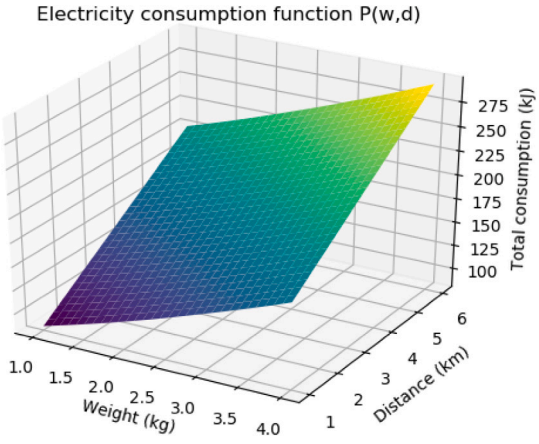

Fig. 1. A representation of the non-linear electricity consumption function.

Note that in this process, we ignore the electricity consumption of service time at customer i, and thus we assume that the service process consumes no electricity during the drone flight. During these six phases of the drone's flight, the drone may carry different parcel weights, travel at different speeds, and require a different amount of time. Thus, the consumed electricity at these phases is of different amounts. To calculate the exact amount of electricity consumption at different phases, the following notations are introduced:

- Drone's vertical take off speed v^t, with unit m/s
- Drone's cruise speed v^c, with unit m/s
- Drone's vertical landing speed v^l, with unit m/s

With this notation, we are ready to introduce the drone's electricity consumption model. There are a variety of electricity consumption models to account for the drone's flight endurance during its trip. The most common approach is to assume that the drone has a fixed endurance, whether measured in time or distance, regardless of the drone's cruising speed and the weight of the parcels it carries. This fixed endurance approach would not be applied in our paper. All the non-fixed endurance models can be divided into two categories: non-linear and linear models. For the rest of this section, we introduce two electricity consumption models of each type applied in RFLPD, formulating two different models.

3.1.1. Non-linear model

One example of the non-linear electricity consumption model is the one proposed in Liu et al. (2017) and later simplified in Murray and Raj (2020). The calculation of the electricity consumption in different phases are:

- Power consumed in the vertical take-off/landing phase:

$$P^{tl}(w, V_{vert}) = k_1(W+w)g\left[\frac{V_{vert}}{2} + \sqrt{(\frac{V_{vert}}{2})^2 + \frac{(W+w)g}{k_2^2}}\right] + c_2((W+w)g)^{3/2} \tag{12}$$

- Power consumed in the cruising phase:

$$P^c(w, V_{air}) = (c_1+c_2)[((W+w)g - c_5(V_{air}cos\alpha)^2)^2 + (c_4V_{air}^2)^2]^{3/4} + c_4(V_{air})^3 \tag{13}$$

where $k_1, k_2, c_1, c_2, c_4, c_5$ are model coefficients whose values were estimated in Liu et al. (2017), as shown in Table 1. In this formula, W is the UAV frame weight, w is the parcel weight, g is the gravitational constant (9.8 m/s^2), V_{vert} is the vertical speed in the taking off or landing phase and V_{air} is the drone's cruising speed. In this way, the total electricity consumed in the drone's whole trip of delivering parcel of weight w from j to i with cruising speed v^c is:

$$P^{tot}(w, j, i) = \tau_j^t P^{tl}(w, v^t) + \tau_{ji}^c P^c(w, v^c) + \tau_i^l P^{tl}(w, v^l) + \tau_i^t P^{tl}(0, v^t) + \tau_{ij}^c P^c(0, v^c) + \tau_j^l P^{tl}(0, v^l) \tag{14}$$

In this paper, similar to the parameter setting in Murray and Raj (2020), we assume the drone's taking-off and landing speed are 7.8 m/s and 3.9 m/s, respectively while the cruising speed is assumed to be 15.5 m/s, which is approximately 35 *mph*. Besides, the cruise altitude is also chosen to be 50 m, per the Federal Aviation Administration's regulation that the maximum allowed altitude is 400 ft (122 m) above ground level. In this way, the required taking-off time τ^t and landing time τ^l are fixed values. With fixed cruising speed, now the electricity consumption $P^{tot}(w, j, i)$ is a function of two decision variables: parcel weight w_i and distance between facility j and customer i, which is d_{ji}. A representation of this multi-variable function is shown in Fig. 1.

When this non-linear function is used to model drones' electricity consumption in RFLPD, directly incorporating the function into the constraint (8) would apparently makes the problem intractable. However, as both the drone cruising speed and distance

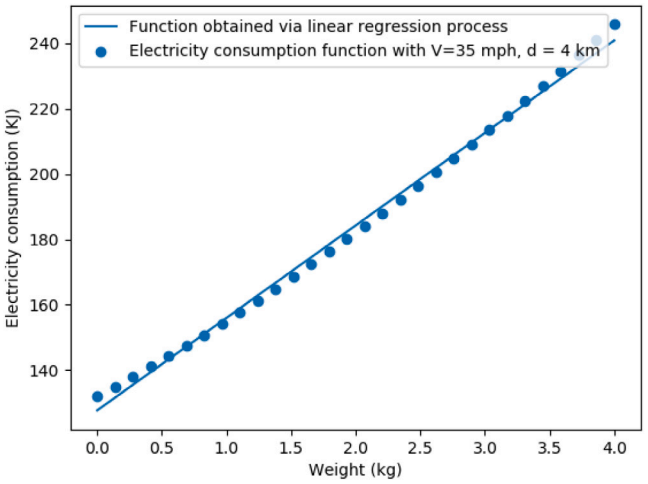

Fig. 2. A comparison between original consumption function and linear regression result.

Table 1
Coefficient values for the non-linear and linear model.

Coefficient	Value (unit)
k_1	0.8554
k_2	0.3051 ($\sqrt{\text{kg}}$/m)
c_1	2.8037 ($\sqrt{\text{m}}$/kg)
c_2	0.3177 ($\sqrt{\text{m}}$/kg)
c_4	0.0296 (kg/m)
c_5	0.0279 (Ns/m)
α	10 (degree)
g	9.8 (ms^2)
$m_t + m_b$	10.1 (kg)
$\kappa_s\eta$	6.85

between facility j and customer i are fixed values, the total consumed power can be expressed as a function of w_i only, which is denoted as $P_{ji}^{tot}(w)$. An representation of this function when $V^c = 35$ mph, $d_{ij} = 4$ km is shown in Fig. 2.

To simplify and incorporate this non-linear function into RFLPD-B, with each pair of j and i and its corresponding distance d_{ji}, a linear regression process is carried out, to estimate the total power consumption of the delivery trip, which includes both the service trip and return trip of the drone. The estimated linear function is denoted as $\tilde{P}_{ji}^{tot}(w)$, with the form

$$\tilde{P}_{ji}^{tot}(w) = a_{ij}^{1n} + a_{ij}^{2n} w, \ \forall i \in I, j \in J \tag{15}$$

where a_{ij}^{1n} and a_{ij}^{2n} are intercept and coefficient of the estimated function, respectively (letter "n" in the superscript stands for "non-linear") and w represents the weight of the parcel. A comparison of the original function $P_{ji}^{tot}(w)$ and the estimated linear function $\tilde{P}_{ji}^{tot}(w)$ is also shown in Fig. 2. Based on the results obtained from the numerical analysis section, the average goodness-of-fit (R-squared) value of the linear regression results are 99.6%.

With the linear regression result, we can incorporate $\tilde{P}_{ji}^{tot}(w)$ into constraints (8), which now can be represented as

$$\sum_i [a_{ij}^{1n} + a_{ij}^{2n}(1 + \theta_i s_i) w_i] x_{ijk} \le B z_{jk}, \ \forall j \in J, k \in K \tag{16}$$

This model that express constraints (8) in the form of constraints (16) is named RFLPD-BN, where the letters "*BN*" indicate binary x variables and a nonlinear electricity consumption model.

3.1.2. Linear model

Unlike the non-linear model, a linear electricity consumption model assumes that the power consumption rate at different phases (taking off, cruising, landing) are the same, and thus the total electricity consumed can be expressed as a linear function. Some examples of linear models include the one proposed in Dorling et al. (2017) and the one presented in Figliozzi (2017). In particular, Figliozzi (2017) expressed the total electricity consumed to deliver an item whose weight is χ from facility j to customer i as:

$$b_{ij}(\chi) = \frac{(m_t + m_b + \chi)g}{\kappa_s \eta} d_{ij} + \frac{(m_t + m_b)g}{\kappa_s \eta} d_{ji}, \forall i \in I, j \in J \tag{17}$$

Table 2
A list of all models mentioned in the paper.

Model Name	Model description	Model purpose
RFLPD-BN	Binary model that adopts an estimation of nonlinear function (14)	Practical use
RFLPD-BL	Binary model that adopts linear function (17)	Practical use
RFLPD-C	Continuous model that adopts simplified function (20)	Practical use
"ideal" continuous	A theoretical continuous model that adopts discontinuous function (19)	Comparison only
RFLPD-BS	Binary model that adopts simplified function (20)	Comparison only
RFLPD-CL	Continuous model that adopts linear function (17)	Comparison only

where η is the drone's power transfer efficiency, κ_s is the lift to drag ratio, m_b is the drone's battery mass, m_t is the drone's tare mass (without battery and package) and g is acceleration due to gravity. The default values of these parameters are shown in Table 1. In this way, the total electricity consumption of the trip is a linear function of the parcel weight and the distance between the facility and the customer.

Function (17) can be incorporated into constraints (8) directly, transforming it to

$$\sum_{i\in I}[a_{ij}^{1l}+a_{ij}^{2l}(1+\theta_i s_i)w_i]x_{ijk}\le Bz_{jk},\ \forall j\in J,k\in K \tag{18}$$

where $a_{ij}^{1l}=\frac{2(m_t+m_b)gd_{ij}}{\kappa_s\eta}$ and $a_{ij}^{2l}=\frac{gd_{ij}}{\kappa_s\eta}$ and letter "l" in the superscript stands for "linear". The model where that express constraints (8) in the form of constraints (18) is named as RFLPD-BL.

3.2. Models allowing split delivery

In the previous two models, second-stage decision variables x_{ijk} are assumed to be binary, which indicates that customers must be fully served by a single drone and deliveries cannot be split. This restriction on the way customers can be served may lead to high penalty costs. For example, when the actual demand of customer i exceeds the drone's capacity, this assumption indicates that the customers' demand would never be satisfied at any portion, which results in high penalty costs. Thus, in this section, we try to relax the "no split delivery" assumption by enabling x_{ijk} to be continuous in an attempt to improve the flexibility and efficiency of the operational stage; for many products distributed during a disaster (food, medication, blood, etc.) it is reasonable to assume demand can be satisfied through multiple smaller deliveries.

When the linear function is used to model drone's electricity consumption and x_{ijk} is continuous, directly adopting this consumption function would lead to

$$b_{ij}(x_{ijk})=\begin{cases}0 & \text{if } x_{ijk}=0,\forall\ i\in I,j\in J,k\in K\\ a_{ij}^{1l}+a_{ij}^{2l}(1+\theta_i s_i)w_i x_{ijk} & \text{otherwise}\end{cases} \tag{19}$$

which we will term the "ideal" consumption function for split delivery. Compared to the consumption function when x_{ijk} is binary

$$b_{ij}(x_{ijk})=[a_{ij}^{1l}+a_{ij}^{2l}(1+\theta_i s_i)w_i]x_{ijk}\ \forall i\in I,j\in J,k\in K$$

we notice that the intercept a_{ij}^{1l} in the first function is incurred whenever $x_{ijk}>0$. This is because this positive intercept a_{ij}^{1l} represents the fixed cost associated with transporting the drone'stare and battery mass.

However, it is difficult to incorporate function (19) into the RFLPD model, because this discontinuous function has different forms based on the value of x_{ijk}, which is the decision variable of the model. For this reason, we propose another model that uses a simplified version of (19):

$$b_{ij}(\chi)=\frac{(2\alpha_i+1)g\chi}{\kappa_s\eta}d_{ij},\ \forall\ \ i\in I,j\in J \tag{20}$$

where α_i is a parameter related to customer i. This function assumes that $m_t+m_b=\alpha_i\chi,\ \forall i\in I$ always holds, by assuming for each customer i that drone k visits, the weight of parcel drone k carries is a fixed value. Obviously, the effectiveness of the simplified function depends on the value of α_i. To ensure the final solution obtained by the simplified model remains feasible for the "ideal" model (which we take to be a truer representation), we adopts a conservative approach when estimating the value of α_i. Empirically, we find the simplified model renders reasonable results when $\alpha_i=\frac{2(m_t+m_b)}{E(\tilde{w}_i)}$ where $E(\tilde{w}_i)$ is the expected demand when $\sum_{i\in I}s_i=\Gamma$ and can be calculated as

$$E(\tilde{w}_i)=(1+\theta_i)w_i\frac{\Gamma}{|I|}+w_i\left(1-\frac{\Gamma}{|I|}\right),\ \forall i\in I \tag{21}$$

By replacing b_{ij} with Eq. (20), now constraints (8) can be represented as:

$$\sum_i a_{ij}^{3}(1-\theta_i s_i)w_i x_{ijk}\le Bz_{jk},\ \forall j\in J,k\in K \tag{22}$$

where $a_{ij}^{3}=\frac{(2\alpha_i+1)gd_{ij}}{\kappa_s\eta}$ and the model that express constraints (8) in the form of constraints (22) while assuming continuous x is named as RFLPD-C.

Using function (20) is less accurate than using the "ideal" function (19), as the former lacks the intercept term in the latter. However, when proper α_i values are chosen, this model can generate a solution that is feasible for the "ideal" model (even if we cannot obtain optimal solutions). In this way, the total cost of RFLPD-C represents an upper bound to that of the "ideal" model. The effectiveness and accuracy of the simplified continuous model RFLPD-C will be analyzed and presented in the numerical analysis section.

We also notice that by using the simplified function, RFLPD-C assumes fixed electricity consumption for each (i, j) pair. This fixed consumption assumption is commonly seen in past FLP literature, for example, Snyder (2006), Xie et al. (2016), Shen et al. (2011). However, almost all past work assumes that the facility can interact with the customers it serves directly. While in this research, the facilities can only interact with the transportation tools (e.g., ground vehicles or drones in our case), and then the transportation tool can serve customers associated with the facilities. This assumption indicates that this research considers allocating transportation tools and assigning customers to transportation tools, which is often ignored in previous FLP-related research. This context-setting is commonly seen in location routing problems (LRPs), especially multi-echelon LRPs, which is a field closely related to FLP. A recent survey of various LRPs is Drexl and Schneider (2015). Meanwhile, in the field of LRP, only a few researchers (e.g., Kahfi et al. (2021), Ziaei and Jabbarzadeh (2021)) solved the multi-period planning problem with a robust optimization approach. Thus, RFLPD-C could be seen as a mixture of multi-stage FLP and LRP models.

3.3. Summary of section

To summarize, in this section, we proposed three models intended for practical use (RFLPD-BN, RFLPD-BL, and RFLPD-C), and mentioned three additional models used for benchmarking and comparison (the "ideal" continuous model, RFLPD-BS, and RFLPD-C). The first model, RFLPD-BN, uses binary variables of x_{ijk} and incorporates the estimated non-linear drone electricity consumption model introduced in Liu et al. (2017) and Murray and Raj (2020). Similarly, the second model, RFLPD-BL, also assumes the decision variables x_{ijk} are binary but incorporates a linear drone electricity consumption model introduced in Figliozzi (2017).

Besides these two binary models, we also mentioned an "ideal" continuous model. This "ideal" continuous model uses the original linear electricity consumption function (19) and enables split delivery by assuming continuous x. However, the electricity consumption function adopted in this model is discontinuous and depends on x. Thus, it is difficult to construct this "ideal" continuous model without other specialized methods. As a compromise, we propose a different continuous model, RFLPD-C, which adopts a simplified electricity consumption function. This model is less accurate compared to the "ideal" continuous model, but it can be constructed easily.

The performance comparison among these models will be presented in the numerical analysis section. The numerical analysis section mentions two additional models, RFLPD-BS and RFLPD-CL. RFLPD-BS adopts the simplified electricity consumption function while assuming binary x_{ijk}, and RFLPD-CL uses the original linear electricity consumption function but assumes continuous decision variables. These two models are relatively inaccurate but facilitate comparison of the binary and continuous models so that we can have an immediate sense of how the different electricity consumption functions, and use of continuous x, affect the overall result of RFLPD models.

A summary of all the models mentioned is shown in Table 2, which highlights the difference among these models.

4. Solution method

The solution methods for the binary models (RFLPD-BN, RFLPD-BL) and continuous model (RFLPD-C) are similar, dualizing the inner maximization subproblem or its LP relaxation. The difference between the two solution methods lies in how the significant scenarios are generated. Thus, in this section, we first introduce the exact solution method for RFLPD-C. The solution method for RFLPD-BN and RFLPD-BL will be explained later with minor changes to the former one.

4.1. Solution method for RFLPD-C

For RFLPD-C, the second stage problem involves solving a max–min problem. However, as the inner minimization subproblem is LP, dualizing this subproblem would result in a max–max problem, which also means that the second-stage problem could be solved as a single maximization problem. For this reason, we will first derive the dual formulation of the inner minimization problem of RFLPD-C's second stage problem. Denote the dual variables for constraints (6), (7), (22), (9), (10) and (11) as u_{ijk}, v_i, π_{jk}, o_j, τ_{ijk} and ϕ_{ijk}, respectively. After incorporating the dual formulation of the inner minimization problem, the second-stage problem is:

DualSubP-C:

$$\max_{s,u,v,\pi,o,\phi} \sum_i \sum_j \sum_k y_j u_{ijk} + \sum_i v_i + \sum_j \sum_k B z_{jk} \pi_{jk} + \sum_j U y_j o_j + \sum_i \sum_j \sum_k C_k \tau_{ijk} + \sum_i \sum_j \sum_k \phi_{ijk} + \sum_i r_i w_i (1 + \theta_i s_i) \tag{23}$$

s.t.

$$u_{ijk} + v_i + a_{ij}^3 (1 + \theta_i s_i) w_i \pi_{jk} + (1 + \theta_i s_i) w_i o_j + (1 + \theta_i s_i) w_i \tau_{ijk} + \phi_{ijk} \le (c_{ij} - r_i)(1 + \theta_i s_i) w_i, \qquad \forall i \in I, j \in J, k \in K \tag{24}$$

$$\sum_i s_i \le \Gamma \tag{25}$$

$$u_{ijk}, v_i, \pi_{jk}, o_j, \phi_{ijk} \le 0 \qquad \forall i \in I, j \in J, k \in K \tag{26}$$

$$0 \le s_i \le 1 \qquad \forall i \in I \tag{27}$$

Since in constraint (24) there exists the multiplication of two variables, we replaced the product $s_i o_j$ with a new variable λ_{ij}, $s_i \pi_{jk}$ with a new variable ρ_{ijk} and $s_i \tau_{ijk}$ with a new variable q_{ijk}. Then the big-M method is used to reformulate the problem. Finally, the MILP formulation of the second-stage problem is as follows, where M and $-M$ are the upper and lower bounds for λ_{ij}, ρ_{ij} and q_{ijk}.

SubP-C:

$$\max_{s,u,v,\pi,o,\phi,\lambda,\rho} \sum_i \sum_j \sum_k y_j u_{ijk} + \sum_i v_i + \sum_j \sum_k B z_{jk} \pi_{jk} + \sum_j U y_j o_j + \sum_i \sum_j \sum_k C_k \tau_{ijk} + \sum_i \sum_j \sum_k \phi_{ijk} + \sum_i r_i w_i (1 + \theta_i s_i) \tag{28}$$

s.t.

$$u_{ijk} + v_i + a_{ij}^3 w_i \pi_{jk} + \theta_i a_{ij}^3 w_i \rho_{ijk} + w_i o_j + \theta_i w_i \lambda_{ij} + w_i \tau_{ijk} + \theta_i w_i q_{ijk} + \phi_{ijk} \le (c_{ij} - r_i)(1 + \theta_i s_i) w_i, \qquad \forall i \in I, j \in J, k \in K \tag{29}$$

$$\sum_i s_i \le \Gamma \tag{30}$$

$$\lambda_{ij} \ge o_j \qquad \forall i \in I, j \in J \tag{31}$$

$$\lambda_{ij} \le o_j + M(1 - s_i) \qquad \forall i \in I, j \in J \tag{32}$$

$$\lambda_{ij} \ge -M s_i \qquad \forall i \in I, j \in J \tag{33}$$

$$q_{ijk} \ge \tau_{ijk} \qquad \forall i \in I, j \in J, k \in K \tag{34}$$

$$q_{ijk} \le \tau_{ijk} + M(1 - s_i) \qquad \forall i \in I, j \in J, k \in K \tag{35}$$

$$q_{ijk} \ge -M s_i \qquad \forall i \in I, j \in J, k \in K \tag{36}$$

$$\rho_{ijk} \ge \pi_{jk} \qquad \forall i \in I, j \in J, k \in K \tag{37}$$

$$\rho_{ijk} \le \pi_{jk} + M(1 - s_i) \qquad \forall i \in I, j \in J, k \in K \tag{38}$$

$$\rho_{ijk} \ge -M s_i \qquad \forall i \in I, j \in J, k \in K \tag{39}$$

$$u_{ijk}, v_i, \pi_{jk}, \rho_{ijk}, o_j, \phi_{ijk}, \lambda_{ij}, q_{ijk}, \tau_{ijk} \le 0 \qquad \forall i \in I, j \in J, k \in K \tag{40}$$

$$0 \le s_i \le 1 \qquad \forall i \in I \tag{41}$$

Now, we are ready to present the solution algorithms for RFLPD-C. First, the column-and-constraint generation algorithm is introduced, followed by the Benders decomposition method.

4.1.1. Column-and-constraint generation algorithm

The column-and-constraint generation (C&CG) algorithm was first introduced in Zeng and Zhao (2013) as a solution method to tackle two-stage robust optimization problems. In two-stage robust optimization problems, the second-stage recourse problem is to identify the worst-case scenario among all the possible realizations. So, if the uncertainty set is a finite discrete set, the RO problem can be reformulated as a large-scale problem that enumerates all the possible scenarios. This method is not applicable when the uncertainty set is infinite or very large. However, we could still solve the large-scale problem with a partial enumeration of scenarios by accounting for the important ones. By identifying extreme points of the uncertainty set and adding these critical scenarios into the large-scale problem iteratively, the algorithm produces better approximations of the feasible region successively until an optimal solution is found. Multiple investigations (Zeng and Zhao, 2013; An et al., 2014) have shown that this cutting-plane-like algorithm performs well in practice. For RFLPD-C, we define the master problem as:

MP-C:

$$\min_{y,z,x,\zeta} \sum_j f_j y_j + \zeta \tag{42}$$

s.t.

$$\sum_j y_j \le p \tag{43}$$

$$z_{jk} \le y_j \qquad \forall j \in J, k \in K \tag{44}$$

$$\sum_j z_{jk} \le 1 \qquad \forall k \in K \tag{45}$$

$$z_{jk}, y_j \in \{0,1\} \qquad \forall j \in J, k \in K \tag{46}$$

$$\sum_i \sum_j \sum_k c_{ij} \tilde{w}_i x_{ijk} + \sum_i r_i \tilde{w}_i (1 - \sum_j \sum_k x_{ijk}) \le \zeta \tag{47}$$

$$x^l_{ijk} \le y_j \qquad \forall i \in I, j \in J, k \in K, l \in L \tag{48}$$

$$\sum_j \sum_k x^l_{ijk} \le 1 \qquad \forall i \in I, l \in L \tag{49}$$

$$\sum_i b_{ij} (\tilde{w}_i x^l_{ijk}) \le B z_{jk} \qquad \forall j \in J, k \in K, l \in L \tag{50}$$

$$\sum_i \sum_k (1 + \theta_i s_i) w_i x^l_{ijk} \le U_j y_j \qquad \forall j \in J, l \in L \tag{51}$$

$$(1 + \theta_i s_i) w_i x^l_{ijk} \le C_k \qquad \forall i \in I, j \in J, k \in K, l \in L \tag{52}$$

$$0 \le x^l_{ijk} \le 1 \qquad \forall i \in I, j \in J, k \in K, l \in L \tag{53}$$

where L is the set that contains the significant scenarios and is initialized to be a null set. In this algorithm, the subproblem is SubP-C described in the previously. Now we are ready to introduce the C&CG algorithm:

- Step 1: Initialize LB $= -\infty$, UB $= +\infty$, scenario set $L = \emptyset$. Denote $|L|$ as the cardinality of set L.
- Step 2: Solve the MP, derive an optimal solution $(\boldsymbol{y}^*_{|L|+1}, \boldsymbol{z}^*_{|L|+1}, \zeta^*_{|L|+1}, \boldsymbol{x}^*_1, \ldots, \boldsymbol{x}^*_{|L|})$. Update LB $= \max\{LB, \boldsymbol{f}\boldsymbol{y}^*_{|L|+1} + \zeta^*_{|L|+1}\}$
- Step 3: Solve the subproblem SubP-B or SubP-C with the first-stage decision variables $(\boldsymbol{y}^*_{|L|+1}, \boldsymbol{z}^*_{|L|+1})$ as derived in Step 2. Denote the objective value of the sub-problem as $\Omega(\boldsymbol{y}^*_{|L|+1}, \boldsymbol{z}^*_{|L|+1})$ and the optimal scenario that attains $\Omega(\boldsymbol{y}^*_{|L|+1}, \boldsymbol{z}^*_{|L|+1})$ as s^{new}. Update UB $= \min\{UB, \boldsymbol{f}\boldsymbol{y}^*_{|L|+1} + \Omega(\boldsymbol{y}^*_{|L|+1}, \boldsymbol{z}^*_{|L|+1})\}$.
- Step 4: If $UB - LB > \epsilon$ where ϵ is the pre-set optimality tolerance and s^{new} is not included in L, create new variables $\boldsymbol{x}^*_{|L|+1}$, add the new optimal scenario into the scenario set L. Add the constraints (43)–(47) associated with new variables $\boldsymbol{x}^*_{|L|+1}$ and s^{new} into MP and return to Step 2. If $UB - LB \le \epsilon$, an ϵ-optimal solution is found and the algorithm terminates.

In this algorithm, $\boldsymbol{f}\boldsymbol{y}^*_{|L|+1} + \zeta^*_{|L|+1}$ is a lower bound for the original problem because it is the optimal solution for a relaxation of the original problem. $\boldsymbol{f}\boldsymbol{y}^*_{|L|+1} + \Omega(\boldsymbol{y}^*_{|L|+1}, \boldsymbol{z}^*_{|L|+1})$ is an upper bound for the original problem because it is a feasible solution of the original problem.

The number of iterations needed by the C&CG algorithm is linear in the number of extreme points of the uncertainty set S (call this number m). This is because the second-stage problem is an LP which is always feasible, regardless of the choice of first-stage decision variables (the "relatively complete recourse" assumption). Proposition 2 of Zeng and Zhao (2013) thus applies to show convergence to the optimal value in $O(m)$ iterations.

The key idea of C&CG is to derive the significant scenario in each iteration and add all the constraints and new second-stage decision variables associated with the new scenario into the master problem. Meanwhile, the upper and lower bound for the problem are associated with the newly generated scenarios. Thus, an alternative is to generate multiple scenarios in every iteration and add all the constraints associated with them into the master problem. Using this approach, we can further speed up the feasible region approximation and have better lower and upper bound at each iteration. For example, in each iteration, after solving the subproblem and obtaining the optimal scenario s^{new}, we could modify s^{new} in some ways to get new scenarios. For example, we can modify disrupted customers with the least nominal demands to non-disrupted ones and modify non-disrupted customers with the highest potential demands to disrupt. Following this approach, multiple new scenarios could be found at each iteration. This idea is generally suitable for large instances when obtaining significant scenarios is time-consuming.

4.1.2. Benders decomposition

Benders decomposition (BD) (Geoffrion, 1972) is one of the most widely used methods for solving problems with complicating variables. This method is based on an iterative sequence of projection, outer linearization, and relaxation and thus is especially suitable for solving multi-stage optimization problems. A thorough literature review of this method could be seen in Rahmaniani et al. (2017).

Similar to the C&CG algorithm, BD works by iteratively exchanging the information derived by solving a master problem and subproblem. A set of feasibility and optimality cuts is gradually added into the master problem to approximate the original problem's feasible region until an optimal solution is found. During this process, obtaining the dual information of the subproblem is a crucial issue. As RFLPD-BL, RFLPD-BN, and RFLPD-C have different second-stage problems, the BD approaches used to solve these two problems are slightly different.

For RFLPD-C, as the sub-problem is an LP, and its optimal dual information is used to generate the optimality cut:

$$\zeta \ge \sum_i \sum_j \sum_k y_j u^*_{ijk} + \sum_i v^*_i + \sum_j \sum_k B z_{jk} \pi^*_{jk} + \sum_j U y_j o^*_j + \sum_i \sum_j \sum_k C_k \tau^*_{ijk} + \sum_i \sum_j \sum_k \phi^*_{ijk} + \sum_i r_i w_i (1 + \theta_i s^*_i) \tag{54}$$

where $s^*, u^*, v^*, \pi^*, o^*, \phi^*$ are the optimal solution of SubP. These cuts are iteratively added to the master problem of Benders decomposition:

MP of BD:

$$\min_{y,z,x,\zeta} \sum_j f_j y_j + \zeta$$

s.t. constraint (43)–(46), (54). When applying this approach, instead of solving the subproblem to optimality and using the optimal dual information to generate optimality cuts, one could also generate multiple feasibility cuts in each iteration. Different such techniques are summarized in Rahmaniani et al. (2017).

4.2. Solution method for RFLPD-BN and RFLPD-BL

Unlike RFLPD-C, whose subproblem of the second-stage problem is a linear program, in RFLPD-BN/RFLPD-BL, the subproblem of the second-stage problem is a mixed-integer linear program. To derive the dual of the second-stage subproblem, its integer constraint should be replaced with a continuous constraint. In this way, now the dual formulation of the LP relaxation of the second-stage subproblem is:

DualSubP-B:

$$\max_{s,u,v,\pi,o,\phi} \sum_i \sum_j \sum_k y_j u_{ijk} + \sum_i v_i + \sum_j \sum_k B z_{jk} \pi_{jk} + \sum_j U y_j o_j + \sum_i \sum_j \sum_k C_k \tau_{ijk} + \sum_i \sum_j \sum_k \phi_{ijk} + \sum_i r_i w_i (1 + \theta_i s_i) \tag{55}$$

s.t.

$$u_{ijk} + v_i + [a^1_{ij} + a^2_{ij}(1 + \theta_i s_i) w_i] \pi_{jk} + (1 + \theta_i s_i) w_i o_j + (1 + \theta_i s_i) w_i \tau_{ijk} + \phi_{ijk} \le (c_{ij} - r_i)(1 + \theta_i s_i) w_i \qquad \forall i \in I, j \in J, k \in K \tag{56}$$

$$\sum_i s_i \le \Gamma \tag{57}$$

$$u_{ijk}, v_i, \pi_{jk}, o_j, \tau_{ijk}, \phi_{ijk} \le 0 \qquad \forall i \in I, j \in J, k \in K \tag{58}$$

$$0 \le s_i \le 1 \qquad \forall i \in I \tag{59}$$

With the same trick used in dealing with RFLPD-C, we also replace the product $s_i o_j$, $s_i \pi_{jk}$ with new variables λ_{ij}, ρ_{ijk}, respectively. After using the big-M method, now the MILP formulation of the second-stage subproblem is as follows, where M and $-M$ are the upper and lower bounds for λ_{ij} and ρ_{ij}.

SubP-B:

$$\max_{s,u,v,\pi,o,\phi} \sum_i \sum_j \sum_k y_j u_{ijk} + \sum_i v_i + \sum_j \sum_k B z_{jk} \pi_{jk} + \sum_j U y_j o_j + \sum_i \sum_j \sum_k C_k \tau_{ijk} + \sum_i \sum_j \sum_k \phi_{ijk} + \sum_i r_i w_i (1 + \theta_i s_i) \tag{60}$$

s.t.

$$u_{ijk} + v_i + (a^1_{ij} + a^2_{ij} w_i) \pi_{jk} + a^2_{ij} \theta_i w_i \rho_{ijk} + w_i o_j + \theta_i w_i \lambda_{ij} + w_i \tau_{ijk} + \theta_i w_i q_{ijk} + \phi_{ijk} \le (c_{ij} - r_i)(1 + \theta_i s_i) w_i \qquad \forall i \in I, j \in J, k \in K \tag{61}$$

$$\sum_i s_i \le \Gamma \tag{62}$$

along with constraints (31)–(40) and domain constraint (59).

To solve RFLPD-BN/RFLPD-BL with the above formulation, we could also adopt the C&CG method. This is because, unlike the Benders decomposition, the C&CG algorithm does not use the dual information of the second-stage problem. Instead, it uses the significant scenarios obtained by solving the second-stage problem and then solves the large-scale MILP in MP. Thus, although in RFLPD-BN/RFLPD-BL, the decision variables in the second-stage problem are binary and no dual information is available for this problem, we could still derive the significant scenarios using the dual of the LP relaxation of the second-stage problem.

However, as the second-stage problem is an integer program, strong duality does not hold. Thus, solving SubP-B exactly does not guarantee an optimal solution for the second-stage problem, and the scenario generated is not guaranteed optimal. Meanwhile, in C&CG algorithm, the new upper bound is updated as $\boldsymbol{f}\boldsymbol{y}^*_{|L|+1} + \Omega(\boldsymbol{y}^*_{|L|+1}, \boldsymbol{z}^*_{|L|+1})$ because the corresponding solution is feasible for the primal minimization problem of RFLPD-BN/RFLPD-BL. However, as the second-stage inner minimization sub-problem is an integer program, the second term $\Omega(\boldsymbol{y}^*_{|L|+1}, \boldsymbol{z}^*_{|L|+1})$ obtained by solving the LP relaxation of the integer programming is a lower bound on the integer solution objective. As a result, the resulting upper bound of the C&CG algorithm is lower than the actual upper bound when the algorithm get close to the optimal solution, and the C&CG algorithm does not guarantee an optimal solution for RFLPD-BN/RFLPD-BL .

Table 3
A list of key parameters used in tests.

Parameter	Meaning	Value
$\|I\|$	number of customers	dedicated by user
Γ	disruption budget	$\lfloor 0.6\|I\| \rfloor$
$\|J\|$	number of all potential facilities	$\lfloor \|I\|/2 \rfloor$
p	maximum number of opened facilities	$\lceil \|I\|/4 \rceil$
U_j	capacity of facility j	15*median(w_i)
f_j	fixed cost of opening facility j	randint(200,500)
w_i	nominal demand value of customer i	randint(1,4)
θ_i	theta value of customer i	random(0,3)
r_i	unit penalty cost of unsatisfied demand of customer i	100
c_{ij}	unit demand transportation cost of customer i from facility j	$5 * d_{ij}$
$\|K\|$	number of available drones	$\lfloor \|I\|/3 \rfloor$
C_k	load capacity of drone k	6 kg
B_k	battery capacity of drone k	777 wh
$m_t + m_b$	tare mass of drone k (including the battery)	10.1 kg
$\kappa_s \eta$	Power transfer efficiency times lift to drag ratio	6.85

Fortunately, the lower bound generated is still valid, and in the first few iterations of the algorithm, the resulting upper bound and scenario can still be used. Thus, we propose a heuristic C&CG algorithm for RFLPD-BN/RFLPD-BL that obtains a feasible solution by constantly improving the lower bound via generating different scenarios manually. For RFLPD-BN/RFLPD-BL, we define the master problem MP-B as the same formulation as MP-C when the constraint (53) is replaced with the binary constraint for x^l_{ijk}. This algorithm is introduced as follows:

- Step 1: Initialize LB $= -\infty$, UB $= +\infty$, scenario set $L = \emptyset$, $noImp = 0$. Denote $|L|$ as the cardinality of set L.
- Step 2: Solve the MP-B, derive an optimal solution $(\boldsymbol{y}^*_{|L|+1}, \boldsymbol{z}^*_{|L|+1}, \zeta^*_{|L|+1}, \boldsymbol{x}^*_1, \ldots, \boldsymbol{x}^*_{|L|})$. Update LB $= \max\{LB, \boldsymbol{f}\boldsymbol{y}^*_{|L|+1} + \zeta^*_{|L|+1}\}$. If LB improves, $noImp = 0$. Else, $noImp := noImp+1$. If $noImp < noImpMax$, where $noImpMax$ is the pre-set parameter indicating the maximal no-improvement iterations, go to Step 3. Otherwise, terminate the algorithm.
- Step 3: Solve the subproblem SubP-B with the first-stage decision variables $(\boldsymbol{y}^*_{|L|+1}, \boldsymbol{z}^*_{|L|+1})$ as derived in Step 2. Denote the objective value of sup-problem as $\Omega(\boldsymbol{y}^*_{|L|+1}, \boldsymbol{z}^*_{|L|+1})$ and the optimal scenario that solves $\Omega(\boldsymbol{y}^*_{|L|+1}, \boldsymbol{z}^*_{|L|+1})$ as s^{new}. Update UB $= \min\{UB, \boldsymbol{f}\boldsymbol{y}^*_{|L|+1} + \Omega(\boldsymbol{y}^*_{|L|+1}, \boldsymbol{z}^*_{|L|+1})\}$. Go to Step 4.
- Step 4: If the new optimal scenario has not been included in set L, add it into L. Else, change the scenario manually and add the modified scenario in L. Create new variables $\boldsymbol{x}^*_{|L|+1}$ and add the constraints (47)–(51) and binary domain constraint associated with new variables $\boldsymbol{x}^*_{|L|+1}$ and s^{new} into MP-B and return to Step 2.

5. Numerical analysis

This section presents a set of numerical analyses of the proposed models. Test data and parameters setting are introduced first. Then, various computational experiments are conducted to test the effectiveness of the proposed solution algorithms and analyze the sensitivity of the proposed RFLPD models on some key input parameters.

As RFLPD assumes that the delivery method only involves drones' operation, whose service area is relatively small compared to traditional commercial trucks, publicly available FLP data sets are not suitable for this research. Thus, randomly generated RFLPD instances are tested.

For each tested instance, the number of customers $|I|$ contained in the instance is an input parameter set by the tester. The number of potential facility locations and available drones are set to be $\lfloor \frac{|I|}{2} \rfloor$ and $\lfloor \frac{|I|}{3} \rfloor$, respectively. All customer locations are randomly generated in a 10 km × 10 km service area. Each customer's nominal demand is randomly generated between 1 kg and 3 kg. Similarly, each customer's θ value is randomly generated between 0 and 3. We assume that the unit transportation cost of customer i is five times the distance between customer i and facility j that serves it. The unit penalty cost of unsatisfied demand is 100 across all customers. For each instance, the disruption budget is $\Gamma = 0.60$ times the number of customers, indicating that 60% of customers would suffer from demand disruption in the worst-case scenario. Besides, all the potential facility locations are randomly generated in the same 10 km × 10 km service area, with fixed cost randomly generated between 200 and 500. The capacity of each facility is assumed to be 15 times the median nominal demand value of all customers. In these experiments, the drone's technical parameters are mostly adopted from Figliozzi (2017). A summary of the parameters is shown in Table 3. All experiments are run on a 3.6 GHz Intel Core i7 desktop with 32 GB RAM.

5.1. Performance comparison between C&CG and Benders decomposition

Two different solution approaches are introduced in the solution method section: C&CG and BD. Both methods decompose the original problem into two separate problems: the master problem and the subproblem. The method then iterates between these two

Table 4
BD and C&CG performance comparison.

$\|I\|$	BD				C&CG			
	Time(s)	Iter	Obj	Opt?	Time(s)	Iter	Obj	Opt?
5	0.408	3.500	1973.706	Y	0.330	2.000	1973.706	Y
8	39.021	181.800	2763.100	Y	0.555	2.000	2763.100	Y
9	45.644	192.000	3268.054	Y	0.600	2.000	3268.054	Y
10	>1800	>2000	N/A	N/A	0.811	2.133	3585.632	Y
15	>1800	>2000	N/A	N/A	1.763	2.000	4357.123	Y
20	>1800	>2000	N/A	N/A	5.143	2.000	4773.345	Y
40	>1800	>2000	N/A	N/A	31.590	2.000	9649.515	Y

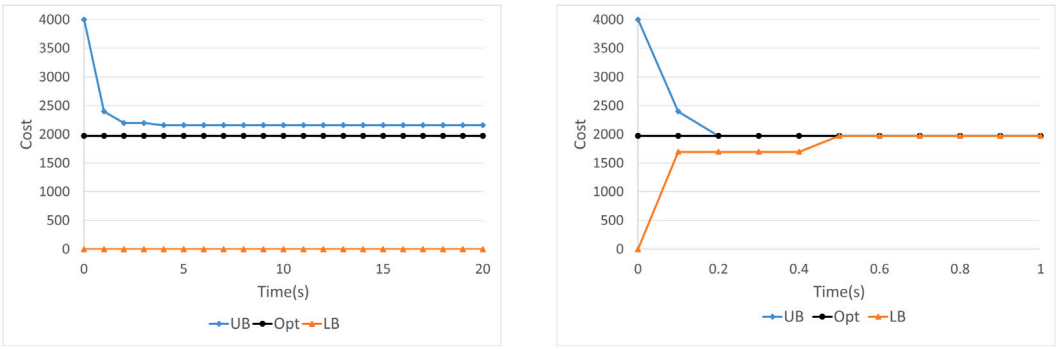

(a) BD converge graph **(b) C&CG converge graph**

Fig. 3. Converge graphs for both algorithms.

problems, aiming to better approximate the feasible region of the original problem in the process. In this subsection, the effectiveness and efficiency of these two methods are tested and compared on the randomly generated instances. Table 4 presents computational results from solving RFLPD-C using Benders decomposition and C&CG algorithm. The values shown in the table are the average result of at least ten independent runs. The following observation can be drawn based on Table 4:

(1) Both methods can obtain the optimal solution for instances with less than ten customers. However, BD fails to converge in 30 min for instances containing more than ten customers. As a comparison, C&CG can obtain an optimal result in about 30 s for instances containing up to 40 customers.
(2) The C&CG algorithm performs much faster than Benders decomposition and terminates in many fewer iterations. These results are consistent with (Zeng and Zhao, 2013) and An et al. (2014). Fig. 3 shows the convergence graph of one of the 8-customer instances for both methods. As can be seen, compared to BD, which makes minimal improvement in the lower bound, the C&CG algorithm can improve both the lower bound and upper bound in a short time and converge to the optimal value.
(3) As in each iteration, a cut is added to BD's master problem, solving the master problem of BD becomes much slower in later stages. BD fails to obtain an optimal solution for instances containing more than ten customers after performing more than 2000 iterations. C&CG is still relatively efficient and can solve instances containing up to 40 customers in 30 s.

5.2. Comparison between RFLPD-BN and RFLPD-BL

This subsection aims to compare the performance of the two binary models, RFLPD-BN and RFLPD-BL, which deploys two different electricity consumption functions when constructing constraints (8). The parameters used in this test are the same as described at the beginning of this section. The test results are illustrated in Table 5, where the numbers shown are the average results of 20 independent runs.

As can be seen from Table 5, in general, the total cost obtained from both models is quite close, although RFLPD-BL has a slightly higher total cost than RFLPD-BN. However, this disparity seems to diminish as the size of the instance grows. This result shows that the two binary models, RFLPD-BN and RFLPD-BL, have a similar total cost, despite using two different electricity consumption models.

5.3. Effectiveness analysis of RFLPD-C

In Section 3, we proposed a continuous model called RFLPD-C, with a less accurate but much simpler electricity consumption function in the drone flight capacity constraints (8). By adopting this simplified consumption function, RFLPD-C can relax the "no-split delivery" assumption and enable a more flexible delivery method, where multiple drones could serve a customer's demand.

Table 5
RFLPD-BN and RFLPD-BL performance comparison.

$\|I\|$	Objective	
	RFLPD-BN	RFLPD-BL
5	3508.10	3599.70
8	5343.18	5466.71
10	7252.525	7319.03
12	8015.92	8033.03
15	10519.00	10528.44
20	13961.72	13968.46

Table 6
A cross performance comparison among four models.

$\|I\|$	RFLPD-BL				RFLPD-BS			
	obj	trans	pen	#feasible	**obj**	trans	pen	#feasible
5	**1986.41**	345.52	1359.00	20/20	**2187.75**	137.03	1777.00	20/20
10	**3280.93**	890.40	1770.00	20/20	**3591.14**	511.87	2439.00	20/20
15	**4469.63**	868.87	3064.00	20/20	**4847.54**	868.87	3064.00	20/20
20	**4730.19**	1534.13	2265.00	20/20	**5275.89**	1115.29	3147.00	20/20
$\|I\|$	RFLPD-CL				RFLPD-C			
	obj	trans	pen	#feasible	**obj**	trans	pen	#feasible
5	**1695.67**	489.57	880.90	1/20	**1951.72**	247.50	1413.26	16/20
10	**2308.88**	1443.57	97.40	0/20	**2781.82**	767.68	1331.44	16/20
15	**2708.34**	1744.25	1.79	0/20	**3151.84**	1362.64	785.91	14/20
20	**3150.49**	1916.52	140.96	0/20	**3706.64**	1414.07	946.28	14/20

This section explores how these two factors (simplifying the consumption function and allowing split delivery) affect the quality and feasibility of the overall solution compared to the binary model RFLPD-BL.

In this section, we conduct a cross-comparison among four different models. The first model is RFLPD-BL, with the original linear electricity consumption function and binary decision variables x_{ijk}. The second model, RFLPD-BS, adopts the simplified electricity consumption function while assuming binary x_{ijk}. The third model is RFLPD-CL, using the original linear electricity consumption function but with continuous second-stage decision variables. The last model is RFLPD-C, which adopts the simplified electricity consumption function and assumes x_{ijk} are continuous. Note that this comparison does not include the RFLPD-BN model, as we think it is unnecessary to include RFLPD-BN when it has a similar overall cost to RFLPD-BL.

The tests use the same parameters as introduced previously. Here, we test instances of four sizes, namely, $|I| = 5, 10, 15, 20$. The test results for four models are summarized in Table 6, where all the results showed are the average value of 20 independent runs. In this table, "*tot*" stands for the total cost of the final solution obtained by the corresponding model, "*trans*" stands for the transportation cost, and "*pen*" represents the total penalty cost of the solution. We also check the feasibility of the obtained solutions of the last three models based on the original linear electricity consumption constraints (18). The number of feasible solutions is shown in the column "*#feasible*". For example, 16/20 in the last column of the first row indicates that in 16 instances, out of a total of 20, the solution obtained by RFLPD-C is feasible in terms of constraints (18).

As can be seen, comparing the final solutions of RFLPD-BL and RFLPD-BS, the latter has a greater total cost in all the test instances. The only difference between these two models is that the latter uses a linear simplified electricity consumption function (20), while the former one uses the original linear function (17). Although RFLPD-BS adopts the simplified electricity consumption function, the feasibility check of its final solutions shows that all the solutions obtained in RFLPD-BS are feasible for RFLPD-BL. Besides, the overall cost of RFLPD-BS is slightly higher than RFLPD-BL. This result shows that the simplified electricity consumption function is a conservative estimation of the current parameter setting's original linear electricity consumption function.

Meanwhile, the results of RFLPD-BL and RFLPD-CL indicate that the final solution of the latter model is about 29% lower than that of the former in terms of the total cost. Note that both models use the original linear electricity consumption function (17), and the only difference is that RFLPD-BL assumes binary x while RFLPD-CL assumes continuous x. Based on this result, it is obvious that the more flexible delivery assignment in the continuous model can achieve a much lower total cost. In particular, when a customer's actual demand exceeds the drone's load capacity, it cannot be served at all in the binary model. In the continuous model, this customer could be partially or even fully served in multiple drone visits. However, the biggest drawback of RFLPD-CL is its feasibility issue. This is because assuming continuous x while using function (17), when the correct form is function (19), clearly underestimates drones' electricity consumption along their routes. As shown in the table, almost all the obtained solutions of RFLPD-CL are infeasible when the most realistic electricity consumption function is used.

Table 6 also shows that the total cost of RFLPD-C, which assumes continuous x and adopts simplified electricity consumption function, lies in between RFLPD-BL and RFLPD-CL. Overall, the total cost of RFLPD-C is about 17% lower than RFLPD-BL. This indicates that although RFLPD-C uses a conservative approach to simplify the electricity consumption function, which tends to overestimate the electricity consumption, the solution obtained by RFLPD-C has a significantly lower total cost by assuming continuous x and enabling split delivery. Besides, most RFLPD-C solution are feasible based on the original linear electricity

Table 7
RFLPD and deterministic FLPD performance comparison.

		RFLPD-BL			One-stage FLPD			Two-stage FLPD		
$\|I\|$	p	**obj**	fac_cost	oper_cost	**obj**	fac_cost	oper_cost	**obj**	fac_cost	oper_cost
$\|I\| = 10$	100	**1873.32**	718.20	1155.11	**2390.56**	329.00	2061.56	**1918.15**	329.00	1589.14
	200	**1870.16**	632.00	1238.15	**3112.46**	387.60	2724.86	**1984.97**	387.60	1597.36
	300	**3700.95**	602.80	3098.05	**6098.20**	613.00	5485.19	**3886.95**	613.00	3273.95
$\|I\| = 20$	100	**3649.16**	845.00	2804.16	**4580.83**	696.19	3884.62	**3719.50**	696.19	6327.63
	200	**4848.32**	877.00	3971.30	**7142.47**	627.80	6514.67	**5053.36**	627.80	4425.56
	300	**7512.65**	869.40	6643.25	**10185.79**	565.00	9620.79	**7653.30**	565.00	7088.30

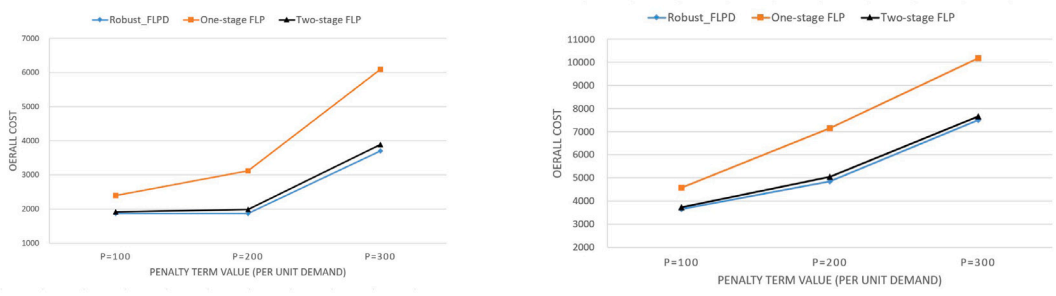

(a) $|I| = 10$ **(b)** $|I| = 20$

Fig. 4. Reliability comparison between RFLPD and FLPD.

consumption constraints (18). This test's results show that RFLPD-C, as a simplification and alternative of the "perfect" model, can still generate a feasible solution whose total cost is much lower than the binary model RFLPD-BL.

5.4. Reliability of RFLPD compared to FLPD

This section aims to show the "reliability" of the RFLPD solution compared to the deterministic FLPD by running a series of simulations. As mentioned before, the robustness of RFLPD is twofold: it makes the facility location plan based on the calculated worst-case scenario of all the possible outcomes in the future, and it can adjust its allocation plan after the actual demand scenario is revealed. On the contrary, the deterministic FLPD makes the location–allocation plan in a one-time fashion without considering demand variations in the future. Moreover, when the actual demand is revealed in the operational stage, it lacks the "recourse" strategy to adjust the original allocation plan. Thus, this section aims to show this point and compare the RFLPD solution with the deterministic FLPD solution in different scenarios.

In this section, for each randomly generated instance, we aim to compare the robustness of the solution among three different models: RFLPD-BL model, deterministic one-stage FLPD, and two-stage FLPD. RFLPD-BL model is the binary model introduced in this paper. The deterministic one-stage FLPD models the problem as FLPD with only the nominal demand value of each customer point. This model indicates that the planner does not consider any future demand variations when making the location–allocation plans. The third model, the two-stage FLPD model, is a mixture of the two models mentioned above: it makes the location plan with only the nominal demand value, but it can adjust its allocation plan after the demand value is revealed. Thus, this model does not consider future demand variations when making the location plan, but it is granted extra flexibility by solving the same min-cost problem as in RFLPD-BL with its facility location plan in the second stage. To avoid any confusion, the MILP formulation of the deterministic one-stage and two-stage FLPD is shown in the appendix.

For each instance, after the solution of three models is obtained, a total of m demand scenarios are generated, and we aim to compare the overall cost of three different solutions via numerous simulation runs. When generating demand scenarios, we assume that 60% of customers have their demand deviate from the nominal value. In this way, the overall cost of three problems can be calculated with each simulated scenario.

In this section, two sets of instances with different total customers are tested, namely, $|I| = 10$ and $|I| = 20$. For any given number of customers, 20 random instances are generated. For each instance, $m = 20$ demand scenarios are considered. Three different penalty values are considered to analyze the effect of unit demand penalty terms r of the unsatisfied customers on the overall cost. The test results of average cost are shown in Table 7.

As can be seen from Table 7 and Fig. 4, the average simulation overall cost of RFLPD-BL is significantly less than one-stage FLP and the two-stage FLPD model, in all of the cases with a different number of customers and unit penalty values. Besides, as the penalty value r increases, the disparity between the RFLPD-BL and the deterministic one-stage FLPD models also increases. The same trend can also be seen in the gap between RFLPD-BL and two-stage FLPD. We also notice that the robust FLPD always has greater first-stage facility cost than the other two models, as the robust FLPD model considers the worst scenario when making the

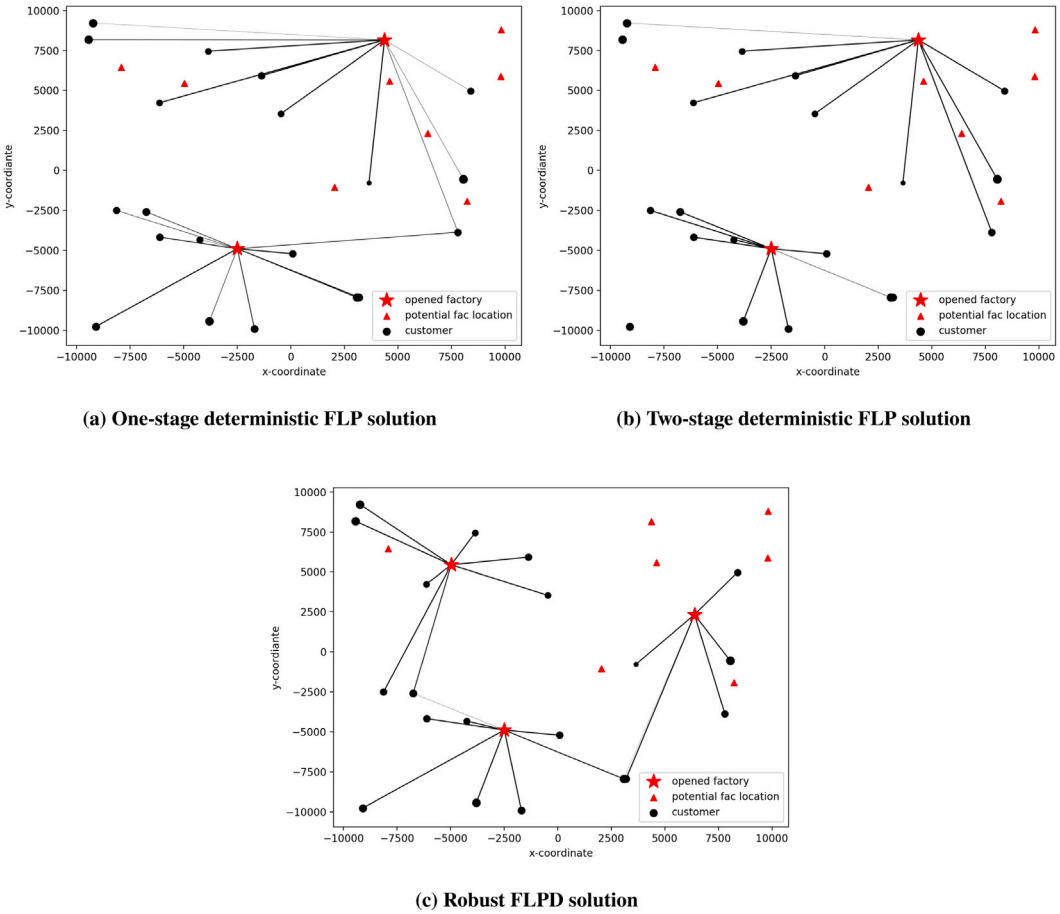

(a) One-stage deterministic FLP solution

(b) Two-stage deterministic FLP solution

(c) Robust FLPD solution

Fig. 5. Simulation result illustration of three different approaches.

location plan. On the other hand, the robust model has significantly less transportation and penalty cost than the other two models in the operational stage.

One thing that is worth mentioning is that these randomly generated demand scenarios are not necessarily the "worst" scenarios whose overall cost is minimized in RFLPD-BL. In fact, these tested demand scenarios might do not even contain the "worst" scenario. Even in this situation, the RFLPD overall average cost is still less than other models. For RFLPD, the increase in overall cost as the penalty value rises seems more "mild" and "robust" than the other two models. Besides, the comparison between RFLPD and two-stage FLPD also shows that even with a second chance to reallocate the resources, it is still beneficial to consider the demand variation when making the location plan in the first planning stage.

Additional simulations are conducted to illustrate the performance of three approaches in the worst possible scenarios. A set of illustrations when $|C| = 20$ are shown in Fig. 5, where the final solution obtained by three different approaches are shown in the same network. In the figure, the size of the customer node indicates its corresponding realized demand, where a bigger-sized dot represents a higher demand. Besides, the thickness of the line indicates the portion of the satisfied demand between an established factory and a customer. Based on Fig. 5, it is evident that the robust model is more conservative in the first location planning stage, can serve more customers, and has a much lower penalty cost than the other two models in the operational stage.

5.5. Effect of demand change budget Γ

The previous section shows that the robustness of the proposed models lies in that they can automatically make a trade-off between the first-stage facility cost and the second-stage operational cost. Specifically, when only a minor disruption might occur, or the penalty of unsatisfied demand is low, the model will spend a relatively small proportion of total cost on the first-stage location plan since it is unnecessary to put a considerable investment to account for the little potential randomness. On the contrary, when the disruption scenario is relatively "severe" or when the penalty of unsatisfied demand is high, the model will build more facilities in the first stage, trying to "prepare" or "alleviate" the future disrupted scenarios. This subsection aims to verify this point by running a sensitivity analysis of the demand change budget Γ on RFLPD-BL. Recall that the demand change budget Γ is an indicator of

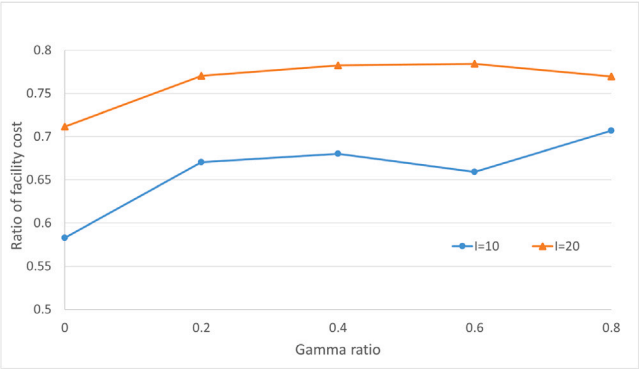

Fig. 6. Sensitivity on demand disruption budget parameter Γ.

the maximum number of customers that could be disrupted simultaneously. When $\Gamma = 0$, the RFLPD is reduced to FLPD. On the other hand, $\Gamma = |I|$ represents that all the customers could be disrupted. Thus, we introduce a new term called gamma ratio $\upsilon = \Gamma/|I| \in [0, 1]$ and test the effect of different values of υ on the relative ratio of facility cost and total cost. The result is shown in Fig. 6, where the vertical axis shows the ratio of the facility cost on the total cost.

As can be seen, for instances of various sizes ($|I| = 10$ and $|I| = 20$), the proportion of the facility cost on the total cost grows as the value of υ increases. For example, when $|I| = 10$, the model spends about 58% of the total cost on the location plan when no disruption is allowed but spends more than 70% of the total cost to account for the future randomness when υ increases to 0.8. This result verifies the trade-offs of the proposed model in different scenarios with various randomness.

6. Conclusion

This paper investigates a newly proposed problem called the two-stage robust facility location problem with drones (RFLPD). This problem assumes that the customers' demands are stochastic and could be disrupted. The planner makes decisions in a two-stage fashion. In the first stage, the planner aims to place facilities in a set of potential locations and assign drones to facilities. In the second stage, the planner needs to allocate customers to the opened facilities and assign drones to serve customers. This model aims to obtain a location–allocation-assignment plan that minimizes a sum of fixed cost, transportation cost, and penalty cost. In this problem, a budget-constrained scenario set describes the uncertainty of customers' demands. Besides, the drone's battery capacity and load capacity are also considered. We first propose two different binary models based on two different drone electricity consumption functions (RFLPD-BL and RFLPD-BN) where no split delivery is allowed in the operational stage. Then to relax the "no split delivery" assumption, the third model, RFLPD-C, is proposed. This model adopts a simplified electricity consumption function but has greater delivery flexibility. For RFLPD-C, two different exact solution methods are proposed: Benders decomposition and column-and-constraint generation. For RFLPD-BL and RFLPD-BN, a modified C&CG method is used to derive a heuristic solution.

In the numerical analysis section, we first compare the performance of the C&CG algorithm and Benders decomposition method and found that the former one is significantly faster than Benders decomposition. Then a comparison between RFLPD-BN and RFLPD-BL indicates that the two models generate a final solution of similar cost, although the total cost obtained by RFLPD-BL is slightly higher. Then an extensive analysis of the effectiveness of RFLPD-C is conducted. Based on the cross-comparison among four models, we found that the simplified electricity consumption function is a conservative estimate of the original linear electricity consumption function. Thus, the results obtained by RFLPD-C could be regarded as an upper bound of the total cost when adopting the "ideal" linear electricity consumption function and enabling split delivery. Furthermore, a reliability comparison via simulation runs among the RFLPD-BL, and two deterministic FLP models show that the RFLPD-BL model has much less total cost in the simulated scenarios, which indicates that it is beneficial to account for future demand variation when making both location–allocation plan and assignment plan. Lastly, a sensitivity analysis on a budget of disruption is also conducted.

This research is the first to consider demand uncertainty in a drone operation-related facility location problem. Besides, the models proposed in this paper are also effective in practical use as they adopt a realistic drone electricity consumption function in the modeling process. Since the robust optimization approach is used in these models, they are especially effective when the penalty cost of unsatisfied customer demand is high.

There are several remaining challenges for this type of problem. Several natural extensions include serving customers in the second operational stage using a truck-drone tandem delivery method, allowing drones to be repositioned to other facilities during the second stage, and considering the uncertainty in the drone's delivery time or facility capacity.

CRediT authorship contribution statement

Tengkuo Zhu: Conceptualization, Methodology, Software, Visualization. **Stephen D. Boyles:** Supervision, Review & editing. **Avinash Unnikrishnan:** Review & editing.

Acknowledgments

This research is based on work supported by the National Science Foundation, United States under Grant No. 1826320/1826337 "Collaborative Research: Real-Time Stochastic Matching Models for Freight Electronic Marketplace", 1562109/1562291 "Collaborative Research: Non-Additive Network Routing and Assignment Models" , 1636154, and 1254921. This work is also supported by the Center for Advanced Multimodal Mobility Solutions and Education (CAMMSE), United States.

Appendix. MIP formulation of deterministic one-stage and two-stage FLPD

The MILP formulation of deterministic FLPD is as follows, with the same notation introduced before.

FLPD:

$$\min_{y,z,x} \sum_j f_j y_j + \sum_i \sum_j \sum_k c_{ij} w_i x_{ijk} + \sum_i r_i w_i (1 - \sum_j \sum_k x_{ijk}) \tag{A.1}$$

s.t.

$$\sum_j y_j \le p \tag{A.2}$$

$$z_{jk} \le y_j \qquad \forall j \in J, k \in K \tag{A.3}$$

$$\sum_j z_{jk} \le 1 \qquad \forall k \in K \tag{A.4}$$

$$z_{jk}, y_j \in \{0,1\} \qquad \forall j \in J, k \in K \tag{A.5}$$

$$x_{ijk} \le y_j \qquad \forall i \in I, j \in J, k \in K \tag{A.6}$$

$$\sum_j \sum_k x_{ijk} \le 1 \qquad \forall i \in I \tag{A.7}$$

$$\sum_i b_{ij}(w_i x_{ijk}) \le B z_{jk} \qquad \forall j \in J, k \in K \tag{A.8}$$

$$\sum_i \sum_k w_i x_{ijk} \le U_j y_j \qquad \forall j \in J \tag{A.9}$$

$$w_i x'_{ijk} \le C_k \qquad \forall i \in I, j \in J, k \in K \tag{A.10}$$

$$x_{ijk} \in \{0,1\} \qquad \forall i \in I, j \in J, k \in K \tag{A.11}$$

For deterministic one-stage FLPD, it uses the above formulation to derive its facility location plan, drone allocation plan (corresponding to decision variables y, z), and drone assignment plan (corresponding to variables x). In the later stage when the demand value is revealed, this model cannot make any changes to the original assignment plan that is made previously.

For the two-stage FLPD model, the above formulation is also used to derive the facility location plan y, drone allocation plan z. However, unlike the one-stage FLPD, the two-stage FLPD can adjust its drone assignment plan x when the actual demand value of each customer point is revealed, based on the established facility location plan. Thus, in the second stage, two-stage FLPD solves the following min-cost problem:

Second-stage FLPD:

$$\min_{x'} \sum_i \sum_j \sum_k c_{ij} w_i x'_{ijk} + \sum_i r_i w_i (1 - \sum_j \sum_k x'_{ijk}) \tag{A.12}$$

s.t.

$$\sum_j y_j \le p \tag{A.13}$$

$$x'_{ijk} \le y_j \qquad \forall i \in I, j \in J, k \in K \tag{A.14}$$

$$\sum_j \sum_k x'_{ijk} \le 1 \qquad \forall i \in I \tag{A.15}$$

$$\sum_i b_{ij}(\tilde{w}_i x'_{ijk}) \le B z_{jk} \qquad \forall j \in J, k \in K \tag{A.16}$$

$$\sum_i \sum_k \tilde{w}_i x'_{ijk} \le U_j y_j \qquad \forall j \in J \tag{A.17}$$

$$\tilde{w}_i x'_{ijk} \le C_k \qquad \forall i \in I, j \in J, k \in K \tag{A.18}$$

$$x'_{ijk} \in \{0,1\} \qquad \forall i \in I, j \in J, k \in K \tag{A.19}$$

In the above formulation, the decision variable x' is the adjusted drone assignment plan and y, z are the parameters that are derived in the first planning phase. For the two-stage FLPD, the final solution is the combined set x', y, z.

References

Agatz, N., Bouman, P., Schmidt, M., 2018. Optimization approaches for the traveling salesman problem with drone. Transp. Sci. 52 (4), 965–981.

AirborneDrones, 2020. High payload drone for delivery & transport. URL https://www.airbornedrones.co/delivery-and-transport.

An, K., Xie, S., Ouyang, Y., 2017. Reliable sensor location for object positioning and surveillance via trilateration. Transp. Res. Procedia 23, 228–245.

An, Y., Zeng, B., Zhang, Y., Zhao, L., 2014. Reliable p-median facility location problem: two-stage robust models and algorithms. Transp. Res. B 64, 54–72.

Ardestani-Jaafari, A., Delage, E., 2018. The value of flexibility in robust location-transportation problems. Transp. Sci. 52 (1), 189–209. http://dx.doi.org/10.1287/trsc.2016.0728.

Atamtürk, A., Zhang, M., 2007. Two-stage robust network flow and design under demand uncertainty. Oper. Res. 55 (4), 662–673. http://dx.doi.org/10.1287/opre.1070.0428.

Balakrishnan, A., Ward, J.E., Wong, R.T., 1987. Integrated facility location and vehicle routing models: Recent work and future prospects. Am. J. Math. Manag. Sci. 7 (1–2), 35–61.

Bloomberg, 2019. Drone package delivery market worth $27.4 Billion by 2030. URL https://www.bloomberg.com/press-releases/2019-12-05/drone-package-delivery-market-worth-27-4-billion-by-2030-exclusive-report-by-marketsandmarkets.

Cappanera, P., Gallo, G., Maffioli, F., 2003. Discrete facility location and routing of obnoxious activities. Discrete Appl. Math. 133 (1–3), 3–28.

Carlsson, J.G., Song, S., 2017. Coordinated logistics with a truck and a drone. Manage. Sci. 64 (9), 4052–4069.

Chauhan, D., Unnikrishnan, A., Figliozzi, M., 2019. Maximum coverage capacitated facility location problem with range constrained drones. Transp. Res. C 99, 1–18.

Chauhan, D.R., Unnikrishnan, A., Figliozzi, M., Boyles, S.D., 2020. Robust maximum coverage facility location problem with drones considering uncertainties in battery availability and consumption. Transp. Res. Rec. 0361198120968094.

Cheng, C., Adulyasak, Y., Rousseau, L.-m., 2021. Robust facility location under disruptions. INFORMS J. Optim. (August).

Choi, Y., Schonfeld, P.M., 2017. Optimization of multi-package drone deliveries considering battery capacity. In: 96th Annual Meeting Of The Transportation Research Board, Washington, DC (Paper No. 17–05769).

Chowdhury, S., Emelogu, A., Marufuzzaman, M., Nurre, S.G., Bian, L., 2017. Drones for disaster response and relief operations: A continuous approximation model. Int. J. Prod. Econ. 188, 167–184.

Correia, I., Saldanha-da Gama, F., 2019. Facility location under uncertainty. In: Location Science. Springer, pp. 185–213.

Cui, T., Ouyang, Y., Shen, Z.-J.M., 2010. Reliable facility location design under the risk of disruptions. Oper. Res. 58 (4-part-1), 998–1011.

Daknama, R., Kraus, E., 2017. Vehicle routing with drones. eprint arXiv:1705.06431. URL https://arxiv.org/pdf/1705.06431.pdf.

Daskin, M.S., Snyder, L.V., Berger, R.T., 2005. Facility location in supply chain design. In: Logistics Systems: Design And Optimization. Springer, pp. 39–65.

Dorling, K., Heinrichs, J., Messier, G.G., Magierowski, S., 2017. Vehicle routing problems for drone delivery. IEEE Trans. Syst. Man Cybern. Syst. 47 (1), 70–85.

Drexl, M., Schneider, M., 2015. A survey of variants and extensions of the location-routing problem. Eur. J. Oper. Res. 241 (2), 283–308.

Drezner, Z., 1987. Heuristic solution methods for two location problems with unreliable facilities. J. Oper. Res. Soc. 38 (6), 509–514.

Dronezone, 2020. Drones for deliveries from medicine to post, packages and pizza. URL https://www.dronezon.com/drones-for-good/drone-parcel-pizza-delivery-service.

Figliozzi, M.A., 2017. Lifecycle modeling and assessment of unmanned aerial vehicles (Drones) CO2e emissions. Transp. Res. D Transp. Environ. 57, 251–261.

Fischetti, M., Polo, C., Scantamburlo, M., 2004. A local branching heuristic for mixed-integer programs with 2-level variables, with an application to a telecommunication network design problem. Netw. Int. J. 44 (2), 61–72.

Geoffrion, A.M., 1972. Generalized benders decomposition. J. Optim. Theory Appl. 10 (4), 237–260.

Golabi, M., Shavarani, S.M., Izbirak, G., 2017. An edge-based stochastic facility location problem in UAV-supported humanitarian relief logistics: a case study of tehran earthquake. Nat. Hazards 87 (3), 1545–1565.

Goodchild, A., Toy, J., 2018. Delivery by drone: An evaluation of unmanned aerial vehicle technology in reducing CO2 emissions in the delivery service industry. Transp. Res. D Transp. Environ. 61, 58–67.

Ha, Q.M., Deville, Y., Pham, Q.D., Hà, M.H., 2018. On the min-cost traveling salesman problem with drone. Transp. Res. C 86, 597–621.

Hajibabai, L., Bai, Y., Ouyang, Y., 2014. Joint optimization of freight facility location and pavement infrastructure rehabilitation under network traffic equilibrium. Transp. Res. B 63, 38–52.

Ilkhanizadeh, S., Golabi, M., Hesami, S., Rjoub, H., 2020. The potential use of drones for tourism in crises: A facility location analysis perspective. J. Risk Financ. Manag. 13 (10), 246.

Kahfi, A., Seyed Hosseini, S.M., Tavakkoli-Moghaddam, R., 2021. A robust optimization approach for a multi-period location-arc routing problem with time windows: A case study of a bank. Int. J. Nonlinear Anal. Appl. 12 (1), 157–173.

Kim, D., Lee, K., Moon, I., 2019. Stochastic facility location model for drones considering uncertain flight distance. Ann. Oper. Res. 283, 1283–1302.

Kim, S.J., Lim, G.J., Cho, J., 2018. Drone flight scheduling under uncertainty on battery duration and air temperature. Comput. Ind. Eng. 117, 291–302.

Kim, H., O'Kelly, M.E., 2009. Reliable p-hub location problems in telecommunication networks. Geogr. Anal. 41 (3), 283–306.

Li, X., Ouyang, Y., 2010. A continuum approximation approach to reliable facility location design under correlated probabilistic disruptions. Transp. Res. B 44 (4), 535–548.

Liu, Z., Sengupta, R., Kurzhanskiy, A., 2017. A power consumption model for multi-rotor small unmanned aircraft systems. In: 2017 International Conference On Unmanned Aircraft Systems. ICUAS, IEEE, pp. 310–315.

Louveaux, F., 1993. Stochastic location analysis: Location science 1, 127-154.. Locat. Sci..

Lu, Z., Bostel, N., 2007. A facility location model for logistics systems including reverse flows: The case of remanufacturing activities. Comput. Oper. Res. 34 (2), 299–323.

Macias, J.E., Angeloudis, P., Ochieng, W., 2020. Optimal hub selection for rapid medical deliveries using unmanned aerial vehicles. Transp. Res. C 110, 56–80.

Melo, M.T., Nickel, S., Saldanha-Da-Gama, F., 2009. Facility location and supply chain management–a review. Eur. J. Oper. Res. 196 (2), 401–412.

Mišković, S., Stanimirović, Z., Grujičić, I., 2017. Solving the robust two-stage capacitated facility location problem with uncertain transportation costs. Optim. Lett. 11 (6), 1169–1184.

Murray, C.C., Chu, A.G., 2015. The flying sidekick traveling salesman problem: Optimization of drone-assisted parcel delivery. Transp. Res. C http://dx.doi.org/10.1016/j.trc.2015.03.005.

Murray, C.C., Raj, R., 2020. The multiple flying sidekicks traveling salesman problem: Parcel delivery with multiple drones. Transp. Res. C 110, 368–398.

Otto, A., Agatz, N., Campbell, J., Golden, B., Pesch, E., 2018. Optimization approaches for civil applications of unmanned aerial vehicles (UAVs) or aerial drones: A survey. Networks 72 (4), 411–458.

Ouyang, Y., Wang, Z., Yang, H., 2015. Facility location design under continuous traffic equilibrium. Transp. Res. B 81, 18–33.

Owen, S.H., Daskin, M.S., 1998. Strategic facility location: A review. Eur. J. Oper. Res. 111 (3), 423–447.

Poikonen, S., Wang, X., Golden, B., 2017. The vehicle routing problem with drones: Extended models and connections. Networks 70 (1), 34–43.

Ponza, A., 2016. Optimization of Drone-Assisted Parcel Delivery. University of Padova.

Pulver, A., Wei, R., 2018. Optimizing the spatial location of medical drones. Appl. Geogr. 90, 9–16.

Rahmaniani, R., Crainic, T.G., Gendreau, M., Rei, W., 2017. The benders decomposition algorithm: A literature review. Eur. J. Oper. Res. 259 (3), 801–817.

Sacramento, D., Pisinger, D., Ropke, S., 2019. An adaptive large neighborhood search metaheuristic for the vehicle routing problem with drones. Transp. Res. C 102, 289–315.
Shavarani, S.M., 2019. Multi-level facility location-allocation problem for post-disaster humanitarian relief distribution: a case study. J. Humanit. Logist. Supply Chain Manag..
Shavarani, S.M., Mosallaeipour, S., Golabi, M., İzbirak, G., 2019. A congested capacitated multi-level fuzzy facility location problem: An efficient drone delivery system. Comput. Oper. Res. 108, 57–68.
Shavarani, S.M., Nejad, M.G., Rismanchian, F., Izbirak, G., 2018. Application of hierarchical facility location problem for optimization of a drone delivery system: a case study of amazon prime air in the city of san francisco. Int. J. Adv. Manuf. Technol. 95 (9–12), 3141–3153.
Shen, Z.-J.M., Zhan, R.L., Zhang, J., 2011. The reliable facility location problem: Formulations, heuristics, and approximation algorithms. INFORMS J. Comput. 23 (3), 470–482.
Snyder, L.V., 2006. Facility location under uncertainty: a review. IIE Trans. 38 (7), 547–564.
UnmannedAirspace, 2020. Drone delivery operations underway in 27 countries. URL https://www.unmannedairspace.info/latest-news-and-information/drone-delivery-operations-underway-in-26-countries.
UnmannedCargo, 2016. How much weight can delivery drones carry. URL http://unmannedcargo.org/how-much-weight-can-delivery-drones-carry/.
Walmart, 2020. Walmart now piloting drone delivery of COVID-19 at-home self-collection kits. URL https://corporate.walmart.com/newsroom/2020/09/22/walmart-now-piloting-drone-delivery-of-covid-19-at-home-self-collection-kits.
Wang, X., Poikonen, S., Golden, B., 2017. The vehicle routing problem with drones: Several worst-case results. Optim. Lett. 11 (4), 679–697.
Xie, S., An, K., Ouyang, Y., 2019. Planning facility location under generally correlated facility disruptions: Use of supporting stations and quasi-probabilities. Transp. Res. B 122, 115–139.
Xie, W., Ouyang, Y., Wong, S.C., 2016. Reliable location-routing design under probabilistic facility disruptions. Transp. Sci. 50 (3), 1128–1138.
Yurek, E.E., Ozmutlu, H.C., 2018. A decomposition-based iterative optimization algorithm for traveling salesman problem with drone. Transp. Res. C 91, 249–262.
Zeng, B., Zhao, L., 2013. Solving two-stage robust optimization problems using a column-and-constraint generation method. Oper. Res. Lett. 41 (5), 457–461.
Zetina, C.A., Contreras, I., Cordeau, J.F., Nikbakhsh, E., 2017. Robust uncapacitated hub location. Transp. Res. B 106, 393–410. http://dx.doi.org/10.1016/j.trb.2017.06.008.
Ziaei, Z., Jabbarzadeh, A., 2021. A multi-objective robust optimization approach for green location-routing planning of multi-modal transportation systems under uncertainty. J. Clean. Prod. 291, 125293.